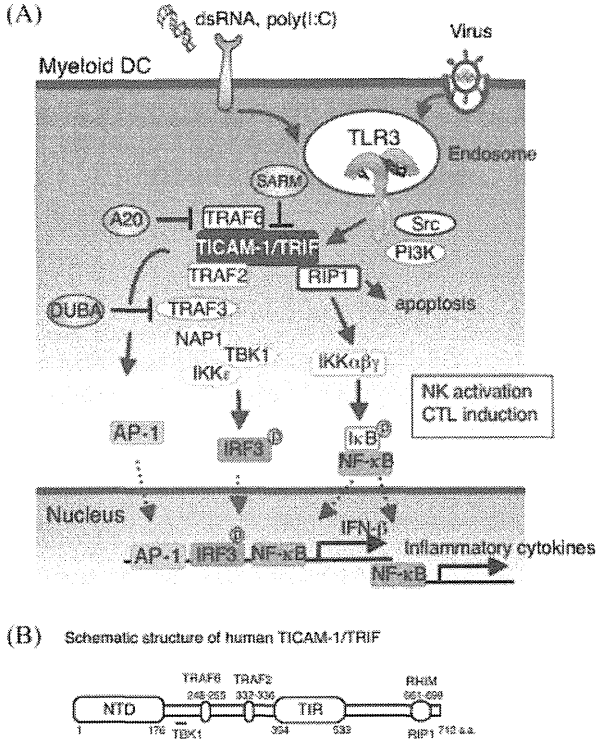

Figure 2. (A) TLR3–TICAM-1-signalling pathway. In myeloid DCs, TLR3 is expressed in the endosomal compartments and recognizes extracellular viral dsRNA and its synthetic analogue poly(I:C). Once TLR3 is dimerized by dsRNA, it recruits the adaptor protein TICAM-1/TRIF that activates the transcription factors, IRF3, NF-κB and AP-1. RIP1 associates with TICAM-1 via the PHIM domain in the C-terminal region and acts as an NF-κB activator and apoptosis mediator in TICAM-1-mediated signalling. TRAF3 and NAP1 participate in the recruitment and activation of the IRF-3 kinases TBK1 and IKKε. Phosphorylated IRF-3 translocates into the nucleus and together with NF-κB and AP-1 induces IFN-β gene transcription. The TICAM-1-mediated AP-1 activation pathway is unclear. (B) Schematic structure of human TICAM-1/TRIF. N-terminal domain (NTD) (1–176 a.a.), TIR domain (394–533 a.a.), RHIM domain (661–699 a.a.), TRAF6-binding site (248–256 a.a.), TRAF2-binding site (332–336 a.a.) and TBK1-binding site (under line) are shown.

TICAM-1 consists of an N-terminal region, a TIR domain and a C-terminal region (Figure 2B). The TIR domain of TICAM-1 is essential for binding to the TIR domain of TLR3 and also to the TLR4 adaptor TICAM-2 (also called TRIF-related adaptor molecule) [59,60]. TICAM-1 is expressed at a low level in most tissues and cells and is diffusely localized in the cytoplasm of resting cells [39]. When endosomal TLR3 is activated by dsRNA, TICAM-1 transiently co-localizes with TLR3, then dissociates from the receptor and forms speckled structures that co-localize with downstream-signalling molecules [39]. Homo-oligomerization through the Pro434 residue in the TIR domain and the C-terminal region is essential for TICAM-1-mediated activation of NF-κB and IRF-3 [61]. Once TICAM-1 is oligomerized, the serine-threonine kinases, TANK-binding kinase 1 (TBK1; also called NAK or T2K) and IkB kinase-related kinase-ε (IKK-ε; also called IKK-i), are activated and phosphorylate IRF-3 [62,63]. The ubiquitin ligase of the TRAF family members, TRAF2, TRAF3 and TRAF6, are downstream-signalling molecules of TICAM-1. TRAF2 and TRAF6 directly bind to the N-terminal region of TICAM-1 [64,65] (Figure 2B). The Lys63-linked autoubiquitination of TRAF3 is required for IRF-3 activation [66,67]. Furthermore, NF-κB-activating kinase (NAK)-associated protein 1 (NAP1) participates in the recruitment of IRF-3 kinases to the N-terminal region of TICAM-1 [68]. Although both TRAF3 and NAP1 associate with oligomerized TICAM-1 and serve as a critical link between TICAM-1 and downstream IRF-3 kinases, there is no evidence that they bind directly to TICAM-1. Interestingly, recent reports showed that direct binding of TBK1 to TICAM-1 is necessary for IRF-3 activation [69]. The Leu194 residue in the N-terminal region is critical for TBK1 binding to TICAM-1. In addition, the Ser189, Arg195 and Ser196 residues are involved in TBK1–TICAM-1 binding.

The N-terminal 176 a.a. of TICAM-1 form a protease-resistant structural domain, designated NTD (Figure 2B). Because the crucial amino acids for TRAF2-, TRAF6- and TBK1-binding reside between the NTD and the TIR domain, naive TICAM-1 may have a closed conformation that covers these binding sites. Indeed, protein–protein interaction analysis revealed that the NTD interacts with the N-terminus of TICAM-1–TIR [69]. Thus, the NTD folds into the TIR domain structure to maintain the naive conformation of TICAM-1. Upon stimulation of TLR3 or TLR4, TICAM-1 oligomerizes through the TIR domain and the C-terminal region, possibly breaking the intramolecular association and inducing a conformational change that allows TBK1 access to TICAM-1.

Whereas the N-terminal region is crucial for TICAM-1-mediated IRF-3 activation, the C-terminal region of TICAM-1 is involved in NF-κB activation and apoptosis. Receptor-interacting protein 1 (RIP1), a kinase containing a death domain, associates with

Copyright © 2011 John Wiley & Sons, Ltd.

DOI: 10.1002/rmv

TICAM-1 via the RIP homotypic interaction motif domain in the C-terminal region and acts as an NF-κB inducer and apoptosis mediator in TICAM-1-mediated signalling [70–72]. TRAF6 has also been implicated in NF-κB activation by TICAM-1 in a cell-type-dependent manner [64,73].

TLR3–TICAM-1-mediated signalling is negatively regulated by a fifth TIR adaptor protein SARM [74]. SARM and TICAM-1 have been shown to interact and SARM strongly suppresses NF-κB activation, as well as IRF-3 activation by TICAM-1. Moreover, deubiquitinating enzyme A (DUBA) negatively regulates TLR3-mediated type I IFN production. DUBA selectively cleaves the Lys63-linked polyubiquitin chains on TRAF3, resulting in its dissociation from the downstream-signalling molecules [75]. In addition, the ubiquitin-modifying enzyme A20 inhibits TICAM-1-mediated NF-κB activation by deubiquitinating TRAF6 [76]. However, the precise mechanisms by which TRAF3 and TRAF6 are ubiquitinated and their interaction with downstream-signalling molecules are unknown.

Antiviral function of TLR3

The role of TLR3 in viral infection is complex (Table 1). Studies in TLR3-deficient ($TLR3^{-/-}$) mice showed that the immune response to different viruses, including lymphocytic choriomeningitis virus (an ambisense RNA virus), vesicular stomatitis virus (a negative-stranded RNA virus), murine cytomegarovirus (MCMV, a dsDNA virus) and reovirus (a dsRNA virus), was unaffected in these mutant mice compared with wild-type mice [77].

By contrast, Hardarson *et al.* [78] reported that TLR3 is important in host defense against encephalomyocarditis virus (EMCV, a positive sense ssRNA virus belonging to the *Picornaviridae* family). When mice were inoculated intraperitoneally with 50 plaque-forming units EMCV, $TLR3^{-/-}$ mice were more susceptible to EMCV infection and had a significantly high viral load in the heart compared with wild-type mice. Opposing to these data, Kato *et al.* [24] showed that MDA5 but not TLR3 plays an important role in host defense against EMCV infection, when mice were infected with 100 plaque-forming units EMCV intraperitoneally. It is unclear why these different results were obtained from similar EMCV infection studies.

Table 1. The role of TLR3 in antiviral responses

	References
Protection	
Flaviviridae [+, ss]	
West Nile virus (WNV)	[84]
Picornaviridae [+, ss]	
Encephalomyocarditis virus (EMCV)	[78]
Poliovirus	[79,80]
Coxsackievirus group B serotype 3 (CVB3)	[82]
Herpesviridae [dsDNA]	
Murine cytomegarovirus (MCMV)	[90]
Herpes simplex virus 1 (HSV-1)	[101]
Deterioration	
Flaviviridae [+, ss]	
West Nile virus (WNV)	[83]
Orthomyxoviridae [−, ss]	
Influenza A virus (IAV)	[88]
Bunyaviridae [−, ss]	
Phlebovirus	[89]

More recently, the essential role of the TLR3–TICAM-1 pathway in protection from poliovirus infection, a virus belonging to the *Picornaviridae* family, has been demonstrated [79,80]. Poliovirus receptor (PVR)-transgenic/TICAM-1-deficient mice are more susceptible than PVR-transgenic mice to intraperitoneal or intravenous inoculation with a low titre of poliovirus [79,80]. Forty-eight hours after infection, virus titres in serum dramatically increased and mortality greatly decreased compared with PVR-transgenic or PVR-transgenic/IPS-1 (RLR adaptor)-deficient mice. It is well known that in cultured mammalian cells, poliovirus infection results in inhibition of cellular protein synthesis so-called 'shut-off' event [81]. Therefore, mRNA upregulation of RIG-I and MDA5 by type I IFN does not link to protein synthesis at an early stage of virus infection. Thus,

Copyright © 2011 John Wiley & Sons, Ltd.

DOI: 10.1002/rmv

it appears that the inhibitory effects of viral multiplication on host cells depend on the TLR3–TICAM-1 pathway, but not the RLR–IPS-1 pathway.

In addition, Negishi *et al.* [82] showed that TLR3$^{-/-}$ mice are more vulnerable to coxsackievirus group B serotype 3 (CVB3, a virus belonging to the *Picornaviridae* family) than wild-type mice, in terms of higher mortality and acute myocarditis. The expression of IL-12p40, IL-1β and IFN-γ mRNAs, but not IFN-β mRNA, was impaired in the hearts of CVB3-infected TLR3-deficient mice compared with those of wild-type mice infected with CVB3. By contrast, expression of TLR3 by transgene protects mice from lethal CVB3 infection and hepatitis even in the absence of type I IFN signalling. Antibody blocking studies revealed that TLR3–TICAM-1-dependent type II IFN (IFN-γ) production is critical for host defense against CVB3 infection [82].

Remarkably, Wang *et al.* [83] demonstrated that TLR3 is involved in the viral pathogenesis of West Nile virus (WNV, a positive-stranded RNA virus). TLR3$^{-/-}$ mice showed impaired cytokine production and enhanced viral loads in the periphery, whereas in the brain, the viral load, inflammatory responses and neuropathology were reduced compared with wild-type mice [83]. TLR3-mediated peripheral inflammatory cytokine production is critical for disruption of the blood–brain barrier, which facilitates viral entry into the brain causing lethal encephalitis. Therefore, TLR3$^{-/-}$ mice are more resistant to lethal WNV infection. In contrast, Daffis *et al.* [84] reported the protective role of TLR3 in sublethal WNV infection. The absence of TLR3 enhances WNV mortality in mice and increases viral burden in the brain after inoculation with the pathogenic New York strain of WNV, although there are little differences in WNV-specific antibody responses, CD8$^+$ T-cell activation, blood–brain barrier permeability and IFN-α/β induction in draining lymph nodes and serum, between wild-type and TLR3$^{-/-}$ mice [84]. The reason why TLR3 shows the opposite function against WNV infection remains to be determined.

In other RNA viral infections such as respiratory syncytial virus, IAV and phlebovirus (all negative-stranded RNA viruses), TLR3-dependent inflammatory cytokine and chemokine production also appears to affect virus-induced pathology and host survival [85–89]. TLR3$^{-/-}$ mice infected with IAV exhibited reduced inflammatory mediators, leading to increased survival [88]. It is notable that experimental conditions using high viral doses may lead to the over-production of inflammatory cytokines and chemokines. However, what type of TLR3-expressing cells that respond to virus-derived dsRNA *in vivo* has not been shown in these studies.

Cellular immunity induced by the TLR3–TICAM-1 pathway

In addition to type I IFNs, CTLs and NK cells are also principal effector cells in antiviral immunity. The contribution of TLR3 to antiviral responses has been shown in MCMV infection [90], during which virus clearance is partly dependent on NK cell activation. TLR3$^{-/-}$ mice are hypersusceptible to MCMV infection. Cytokine (type I IFN, IL-12p40 and IFN-γ) production, and NK cell and NKT cell activation are impaired in TLR3$^{-/-}$ mice compared with wild-type mice.

Selective TLR3 expression in myeloid DCs but not in pDCs raises the possibility that TLR3 also plays a key role in the antiviral response by induction of adaptive immune responses rather than primary IFN-α/β production (Table 2). Myeloid DCs are the most effective professional antigen-presenting cells, possessing several antigen processing and transporting pathways [91,92]. One of the most notable features of myeloid DCs is the cross-presentation of exogenous antigens to CD8$^+$ T cells. This pathway is important for effective host CTL induction against viruses that do not directly infect DCs. Among the myeloid DC subsets, the splenic CD8α$^+$ DC subset in mice and the CD141(BDCA3)$^+$DNGR-1(CLEC9A)$^+$ DC subset in humans highly express TLR3 and display a superior capacity for cross-presenting apoptotic and necrotic cell antigens after TLR3 stimulation [93–97]. Using TLR3-deficient mice, Schultz *et al.* [98] clearly showed that TLR3 plays an important role in cross-priming. Mouse CD8α$^+$ DCs are activated by phagocytosis of apoptotic bodies from virally infected cells or cells containing poly(I:C) in a TLR3-dependent manner. Furthermore, immunization with virally infected cells or cells containing poly(I:C), both carrying ovalbumin antigen, induces ovalbumin-specific CD8$^+$ T-cell responses, which are largely dependent on TLR3-expressing DCs [98]. In many cases, virally infected cells produce IFN-α/β which activates DCs to

Copyright © 2011 John Wiley & Sons, Ltd.

Table 2. Expression of nucleic acid-sensing TLRs in DC subsets

	DC subset	TLR3	TLR7	TLR8	TLR9	References
Human	Myeloid DC					
	MoDC	+	−	+	−	[31–35]
	$CD11c^+CD1c^+$DC	+	−	+	−	[34,35,94,95]
	$CD141^+CLEC9A^+$DC	++	−	+	−	[94,95]
	Plasmacytoid DC	−	+	−	+	[34,35]
Mouse	Myeloid DC					
	BMDC	+	−	−	+	[95]
	$CD8\alpha^+$ DC	++	−	−	+	[93,95]
	Plasmacytoid DC	−	+	−	+	[93,95]

MoDC, monocyte-derived immature dendritic cells; BMDC, bone marrow-derived DC.

promote $CD8^+$ T-cell cross-priming [99]. Thus, both TLR3- and IFN-α/β-mediated signalling are likely implicated in licensing DCs for the cross-priming of $CD8^+$ T cells.

In humans, Ebihara *et al.* [100] demonstrated the role of TLR3, expressed in myeloid DCs, in the immune response to HCV infection. The JFH1 strain of HCV does not directly infect or stimulate myeloid DCs to activate T cells and NK cells, but instead the phagocytosis of HCV-infected apoptotic cells that contain HCV-derived dsRNA and their interaction with the TLR3 pathway in myeloid DCs, plays a critical role in DC maturation and activation of T and NK cells [100]. In addition, Jongbloed *et al.* [94] reported that $CD141^+$ DCs are able to cross-present viral antigens from human cytomegalovirus-infected necrotic fibroblasts. Physiologically, TLR3 in a DC subset specialized for antigen presentation appears to encounter viral dsRNAs in the endosome by uptake of apoptotic or necrotic virus-infected cells and signals for cross-presentation of viral antigens. Furthermore, a dominant-negative TLR3 allele was found in children with herpes simplex virus 1 (HSV-1) encephalitis [101]. TLR3 is expressed in the central nervous system, where it is required to control HSV-1. Interestingly, recent paper demonstrated that mouse $CD8\alpha^+$ DCs and human $CD141^+$ DCs are major producers of IFN-λ in response to poly(I:C), which depends on TLR3 [102]. Thus, TLR3 plays a role in the antiviral response, dependent on the viral genome structure, the route of virus entry into cells, the TLR3-expressing cell type that encounters viral dsRNA, and the properties of the host anti-viral effector functions.

Application of the TLR3 ligand to adjuvant vaccine therapy

Selective expression of TLR3 in myeloid DCs, especially human $CD141^+$ DCs and mouse $CD8\alpha^+$ DC subsets, is the advantage in employing TLR3 ligands as adjuvant. In addition to the TLR3-dependent CTL activation described above, DC-mediated NK cell activation is also important for the adjuvancy of TLR3 ligands. Akazawa *et al.* [103] showed that the TLR3–TICAM-1 pathway is essential for poly(I:C)-induced NK-cell-mediated tumour regression in a syngeneic mouse tumour implant model. Remarkably, production of IFN-α is not impaired in TICAM-$1^{-/-}$ mice compared with wild-type mice after *in vivo* poly(I:C) injection or *in vitro* bone marrow-derived DC (BMDC) stimulation, whereas IL-12 production is completely dependent on TICAM-1, consistent with other reports [22,104]. Furthermore, NK cell activation requires cell–cell contact with BMDCs preactivated by poly(I:C) but not IFN-α or IL-12. Thus, the TLR3–TICAM-1 pathway in myeloid DCs facilitates the DC–NK cell interaction following NK cell activation. TICAM-1–IRF3-dependent expression of a novel molecule, namely IRF-3-dependent NK-activating molecule (INAM), in myeloid DCs is required for NK activation [104]. Poly(I:C)-induced MDA5-dependent myeloid DC activation is also implicated in NK cell activation [105,106].

Copyright © 2011 John Wiley & Sons, Ltd.

DOI: 10.1002/rmv

However, several issues remain unresolved including a suitable transport system for TLR3 ligands. Poly(I:C) injected intraperitoneally in mice activates both TLR3 and MDA5, indicating that extracellular poly(I:C) is delivered to endosomal TLR3 and further to cytosolic MDA5 in murine cells. A recent study demonstrated that CD14 enhances poly(I:C)-mediated TLR3 activation in bone marrow-derived macrophages by directly binding to poly(I:C) and mediating cellular uptake of poly(I:C) [107]. The internalized poly(I:C) then colocalizes with CD14 and TLR3. Since the extracellular domain of CD14 consists of LRRs [108], CD14 may associate with TLR3 and transfer poly(I:C) to TLR3 in macrophage endosomes. In the case of CD14-negative myeloid DCs, extracellular dsRNA must be internalized with the putative uptake receptor. Indeed, it has been demonstrated by our group and others that poly(I:C) is internalized into human monocyte-derived immature DCs and mouse BMDCs via clathrin-dependent endocytosis, and B- and C-type oligodeoxynucleotides share the uptake receptor with poly(I:C) [109]. Notably, among various synthetic dsRNAs, poly(I:C) is preferentially internalized and activates TLR3 in myeloid DCs. By contrast, *in vitro*-transcribed dsRNAs of various lengths (50–1000 bp) cannot be internalized into myeloid DCs [110]. Thus, uptake of TLR3 ligands largely depends on the dsRNA structure recognized by the uptake receptor expressed on myeloid DCs.

The dsRNA structure and the targeting approach of dsRNA to the endosomal TLR3 in the appropriate DC subset, are important factors involved in generating innate and adaptive immune responses by TLR3 ligands. Gowen *et al.* [111] showed that poly(I:C_{12}U) induces IFN-β in a TLR3-dependent and MDA5-independent manner, and exhibits protective anti-viral effects in mice. Identification of the putative dsRNA uptake receptor is crucial for analysing the intracellular transport of dsRNA. Furthermore, clarification of the differences between the RIG-I/MDA5-mediated and TLR3–TICAM-1-mediated signalling pathways is important for assessment of dsRNA-induced immune responses.

Concluding remarks

The protective role of TLR3 in virus infection is now becoming clear from experiments using an infectious mouse model or TLR3-transgenic mice. Since both CVB3 and poliovirus belong to the *Picornaviridae* family, along with encephalomyocarditis virus that is recognized by MDA5, distinct virus properties rather than virus genome structure appear to determine which RNA sensors act in antiviral defense in host cells. The molecular mechanism behind the anti-viral function of TLR3 *in vivo* and the identification of TLR3–TICAM-1-mediated signalling cascades distinct from those of RIG-I/MDA5, are important factors for understanding the role of RNA-sensors in the host defense system. In addition, characterization of a new myeloid DC subset that expresses a high level of TLR3 and has a high capacity to present antigen from apoptotic and necrotic cells after TLR3 activation, may provide insight into the role of TLR3 in the activation of NK cells and CTLs in viral infection. This, in turn, may advance the development of TLR3-related vaccine adjuvants effective against tumours and/or infectious diseases.

REFERENCES

1. Muller U, Steinhoff U, Reis LFL, *et al.* Functional role of type I and type II interferons in antiviral defense. *Science* 1994; **264**: 1918–1921.
2. Vilcek J. Fifty years of interferon research: aiming at a moving target. *Immunity* 2006; **25**: 343–348.
3. Garcia-Sastre A, Biron CA. Type 1 interferons and the virus-host relationship: a lesson in Détente. *Science* 2006; **312**: 879–882.
4. Clemens MJ. PKR-a protein kinase regulated by double-stranded RNA. *International Journal of Biochemistry and Cell Biology* 1997; **29**: 945–949.
5. Samuel CE. Antiviral actions of interferon, interferon-regulated cellular proteins and their surprisingly selective antiviral activities. *Virology* 1991; **183**: 1–11.
6. Yoneyama M, Kikuchi M, Natsukawa T, *et al.* The RNA helicase RIG-I has an essential function in double-stranded RNA-induced innate antiviral responses. *Nature Immunology* 2004; **5**: 730–737.
7. Yoneyama M, Kikuchi M, Matsumoto K, *et al.* Shared and unique functions of the DExD/H-box helicases RIG-I, MDA5, and LGP2 in antiviral innate immunity. *Journal of Immunology* 2005; **175**: 2851–2858.
8. Akira S, Uematsu S, Takeuchi O. Pathogen recognition and innate immunity. *Cell* 2006; **124**: 783–801.
9. Alexopoulou L, Holt AC, Medzhitov R, Flavell RA. RNA and activation of NF-κB by Toll-like receptor 3. *Nature* 2001; **413**: 732–738.
10. Matsumoto M, Kikkawa S, Kohase M, Miyake K, Seya T. Establishment of a monoclonal antibody against human Toll-like receptor 3 that blocks double-stranded RNA-mediated signaling. *Bio-*

Copyright © 2011 John Wiley & Sons, Ltd.

chemical and Biophysical Research Communications 2002; **239**: 1364–1369.
11. Matsumoto M, Seya T. TLR3: interferon induction by double-stranded RNA including poly(I:C). *Advanced Drug Delivery Reviews* 2008; **60**: 805–812.
12. Weber F, Wagner V, Rasmussen SB, Hartmann R, Paludan SR. Double-stranded RNA is produced by positive-stranded RNA viruses and DNA viruses but not in detectable amounts by negative-stranded RNA viruses. *Journal of Virology* 2006; **80**: 5059–5064.
13. Hemmi H, Takeuchi O, Kawai T, *et al.* A Toll-like receptor recognizes bacterial DNA. *Nature* 2000; **408**: 740–745.
14. Heil F, Hemmi H, Hochrein H, *et al.* Species-specific recognition of single-stranded RNA via toll-like receptor 7 and 8. *Science* 2004; **303**: 1526–1529.
15. Diebold SS, Kaisho T, Hemmi H, Akira S, Sousa RC. Innate antiviral responses by means of TLR7-mediated recognition of single-stranded RNA. *Science* 2004; **303**: 1529–1531.
16. Lee HK, Lund JM, Ramanathan B, Mizushima N, Iwasaki A. Autophagy-dependent viral recognition by plasmacytoid dendritic cells. *Science* 2007; **315**: 1398–1401.
17. Hornung V, Ellegast J, Kim S, *et al.* 5′-Triphosphate RNA is ligand for RIG-I. *Science* 2006; **314**: 994–997.
18. Pichlmair A, Schulz O, Tan CP, *et al.* RIG-I-mediated anti-viral responses to single-stranded RNA bearing 5′-phosphates. *Science* 2006; **314**: 997–1001.
19. Schlee M, Roth A, Hornung V, *et al.* Recognition of 5′ triphosphate by RIG-I helicase requires short blunt double-stranded RNA as contained in panhandle of negative-strand virus. *Immunity* 2009; **31**: 25–34.
20. Schmidt A, Schwerd T, Hamm W, *et al.* 5′-triphosphate RNA requires base-paired structures to activate antiviral signaling via RIG-I. *Proceedings of the National Academy of Science of the United States of America* 2009; **106**: 12067–12072.
21. Rehwinkel J, Tan CP, Goubau D, *et al.* RIG-I detects viral genomic RNA during negative-strand RNA virus infection. *Cell* 2010; **140**: 397–408.
22. Kato H, Takeuchi O, Mikamo-Satoh E, *et al.* Length-dependent recognition of double-stranded ribonucleic acids by retinoic acid-inducible gene-I and melanoma differentiation-associated gene 5. *Journal of Experimental Medicine* 2008; **205**: 1601–1610.
23. Kato H, Sato S, Yoneyama M, *et al.* Cell type-specific involvement of RIG-I in antiviral response. *Immunity* 2005; **23**: 19–28.
24. Kato H, Takeuchi O, Sato S, *et al.* Differential roles of MDA5 and RIG-I helicases in the recognition of RNA viruses. *Nature* 2006; **441**: 101–105.
25. Gitlin L, Barchet W, Gilfillan S, *et al.* Essential role of mda-5 in type I IFN responses to polyriboinosinic:polyribocytidylic acid and encephalomyocarditis picornavirus. *Proceedings of the National Academy of Science of the United States of America* 2006; **103**: 8459–8464.
26. Saito T, Owen DM, Jiang F, Marcotrigiano J, Gale M Jr. Innate immunity induced by composition-dependent RIG-I recognition of hepatitis C virus RNA. *Nature* 2008; **454**: 523–527.
27. Rock FL, Hardiman G, Timans JC, Kastelein RA, Bazan JFA. A family of human receptors structurally related to *Drosophila* Toll. *Proceedings of the National Academy of Science of the United States of America* ; **95**: 588–593.
28. Prehaud C, Megret F, Lafage M, Lafon M. Virus infection switches TLR-3-positive human neurons to become strong producers of beta interferon. *Journal of Virology* 2005; **79**: 12893–12904.
29. Farina C, Krumbholz M, Giese T, Hartmann G, Aloisi F, Meinl E. Preferential expression and function of Toll-like receptor 3 in human astrocytes. *Journal of Neuroimmunology* 2005; **159**: 12–19.
30. Town T, Jeng D, Alexopoulou L, Tan J, Flavell RA. Microglia recognize double-stranded RNA via TLR3. *Journal of Immunology* 2006; **176**: 3804–3812.
31. Muzio M, Bosisio D, Polentarutti N, *et al.* Differential expression and regulation of Toll-like receptors (TLR) in human leukocytes: selective expression of TLR3 in dendritic cells. *Journal of Immunology* 2000; **64**: 5998–6004.
32. Visintin A, Mazzoni A, Spitzer JH, Wyllie DH, Dower SK, Segal DM. Regulation of Toll-like receptors in human monocytes and dendritic cells. *Journal of Immunology* 2001; **166**: 249–254.
33. Kadowaki M, Ho S, Antonenko S, *et al.* Subsets of human dendritic cell precursors express different Toll-like receptors and respond to different microbial antigens. *Journal of Experimental Medicine* 2001; **194**: 863–870.
34. Hornung V, Rothenfusser S, Britisch S, *et al.* Quantitative expression of Toll-like receptor 1-10 mRNA in cellular subsets of human peripheral blood mononuclear cells and sensitivity to CpG oligodeoxynucleotides. *Journal of Immunology* 2002; **168**: 4531–4537.
35. Matsumoto M, Funami K, Tanabe M, *et al.* Subcellular localization of Toll-like receptor 3 in human dendritic cells. *Journal of Immunology* 2003; **171**: 3154–3162.
36. Cario E, Podolsky DK. Differential alteration in intestinal epithelial cell expression of Toll-like receptor 3 (TLR3) and TLR4 in inflammatory bowel disease. *Infection and Immunity* 2000; **68**: 7010–7017.
37. Niimi K, Asano Y, Shiraishi T, *et al.* TLR3-mediated synthesis and release of eotaxin-1/CCL11 from human bronchial smooth muscle cells stimulated with double-stranded RNA. *Journal of Immunology* 2007; **178**: 489–495.
38. Nakamura M, Funami K, Komori A, *et al.* Increased expression of Toll-like receptor 3 in intrahepatic bilinary epithelial cells at sites of ductular reaction in diseased livers. *Hepatology International* 2008; **2**: 222–230.
39. Funami K, Sasai M, Ohba Y, Oshiumi H, Seya T, Matsumoto M. Spatiotemporal mobilization of Toll-IL-1 receptor domain-containing adaptor molecule 1 in response to dsRNA. *Journal of Immunology* 2007; **179**: 6867–6872.
40. Funami K, Matsumoto M, Oshiumi H, Akazawa T, Yamamoto A, Seya T. The cytoplasmic 'linker region' in Toll-like receptor 3 controls receptor localization and signaling. *International Immunology* 2004; **16**: 1143–1154.
41. Nishiya T, Kajita E, Miwa S, DeFranco A. TLR3 and TLR7 are targeted to the same intracellular compartments by distinct regulatory elements. *Journal of Biological Chemistry* 2005; **280**: 37107–37117.
42. Miettinen M, Sareneva T, Julkunen I, Matikainen S. IFNs activate toll-like receptor gene expression in viral infections. *Genes and Immunity* 2001; **2**: 349–355.
43. Heinz S, Haehnel V, Karaghiosoff M, *et al.* Species-specific regulation of Toll-like receptor 3 genes in men and mice. *Journal of Biological Chemistry* 2003; **24**: 21502–21509.
44. Tanabe M, Taniguchi M, Takeuchi K, *et al.* Mechanism of up-regulation of human Toll-like receptor (TLR) 3 secondary to infection of measles virus attenuated strains. *Biochemical and Biophysical Research Communications* 2003; **311**: 39–48.
45. Gay NJ, Gangloff M, Weber ANR. Toll-like receptors as molecular switches. *Nature Reviews. Immunology* 2006; **6**: 693–698.

Copyright © 2011 John Wiley & Sons, Ltd.

46. Bell JK, Mullen GED, Leifer CA, Mazzoni A, Davies DR, Segal DM. Leucine-rich repeats and pathogen recognition in Toll-like receptors. *Trends in Immunology* 2003; **24**: 528–533.
47. Choe J, Kelker MS, Wilson IA. Crystal structure of human Toll-like receptor 3 (TLR3) ectodomain. *Science* 2005; **309**: 581–585.
48. Bell JK, Botos I, Hall PR, *et al.* The molecular structure of the Toll-like receptor 3 ligand-binding domain. *Proceedings of the National Academy of Science of the United States of America* 2005; **102**: 10976–10980.
49. Bell JK, Askins J, Hall PR, Davies DR, Segal DM. The dsRNA binding site of human Toll-like receptor 3. *Proceedings of the National Academy of Science of the United States of America* 2006; **103**: 8792–8797.
50. Fukuda K, Watanabe T, Tokisue T, *et al.* Modulation of double-stranded RNA recognition by the N-terminal histidine-rich region of the human Toll-like receptor 3. *Journal of Biological Chemistry* 2008; **283**: 22787–22794.
51. Pirher N, Ivicak K, Pohar J, Bencina M, Jerala R. A second binding site for double-stranded RNA in TLR3 and consequences for interferon activation. *Nature Structural and Molecular Biology* 2008; **15**: 761–763.
52. Leonard JN, Ghirlando R, Askins J, *et al.* The TLR3 signaling complex forms by cooperative receptor dimerization. *Proceedings of the National Academy of Science of the United States of America* 2008; **105**: 258–263.
53. Liu L, Botos I, Wang Y, *et al.* Structural basis of Toll-like receptor 3 signaling with double-stranded RNA. *Science* 2008; **320**: 379–381.
54. Rana TM. Illuminating the silence: understanding the structure and function of small RNAs. *Nature Reviews. Molecular Cell Biology* 2007; **8**: 23–36.
55. Oshiumi H, Matsumoto M, Funami K, Akazawa T, Seya T. TICAM-1, an adaptor molecule that participates in Toll-like receptor 3-mediated interferon-β induction. *Nature Immunology* 2003; **4**: 161–167.
56. Yamamoto M, Sato S, Hemmi H, *et al.* Role of adaptor TRIF in the MyD88-independent Toll-like receptor signaling pathway. *Science* 2003; **301**: 640–643.
57. Johnsen IB, Nguyen TT, Ringdal M, *et al.* Toll-like receptor 3 associates with c-Src tyrosine kinase on endosomes to initiate antiviral signaling. *EMBO Journal* 2006; **25**: 3335–3346.
58. Sarker SN, Peters K, Elco CP, Sakamoto S, Pal S, Sen GC. Novel roles of TLR3 tyrosine phosphorylation and PI3 kinase in double-stranded RNA signaling. *Nature Structural and Molecular Biology* 2004; **11**: 1060–1067.
59. Oshiumi H, Sasai M, Shida K, Fujita T, Matsumoto M, Seya T. TIR-containing adapter molecule (TICAM)-2, a bridging adapter recruiting to Toll-like receptor 4 TICAM-1 that induces interferon-β. *Journal of Biological Chemistry* 2003; **278**: 49751–49762.
60. Fitzgerald KA, Rowe DC, Barnes BJ, *et al.* LPS-TLR4 signaling to IRF-3/7 and NF-κB involves the toll adapters TRAM and TRIF. *Journal of Experimental Medicine* 2003; **198**: 1043–1055.
61. Funami K, Sasai M, Oshiumi H, Seya T, Matsumoto M. Homo-oligomerization is essential for Toll/IL-1 receptor domain-containing adaptor molecule-1 mediated NF-κB and IRF-3 activation. *Journal of Biological Chemistry* 2008; **283**: 18283–18291.
62. Sharma S, tenOever BR, Grandvaux N, Zhou GP, Lin R, Hiscott J. Triggering the interferon antiviral response through an IKK-related pathway. *Science* 2003; **300**: 1148–1151.
63. Fitzgerald KA, McWhirter SM, Faia KL, *et al.* IKKε and TBK1 are essential components of the IRF3 signaling pathway. *Nature Immunology* 2003; **4**: 491–496.
64. Sato S, Sugiyama M, Yamamoto M, *et al.* Toll/IL-1 receptor domain-containing adaptor-inducing IFN-β (TRIF) associates with TNFR-associated factor 6 and TANK-binding kinase 1, and activates two distinct transcription factors, NF-κB and IFN-regulatory factor 3, in the Toll-like receptor signaling. *Journal of Immunology* 2003; **171**: 4304–4310.
65. Sasai M, Tatematsu M, Oshiumi H, *et al.* Direct binding of TRAF2 and TRAF6 to TICAM-1/TRIF adaptor participates in activation of the Toll-like receptor 3/4 pathway. *Molecular Immunology* 2010; **47**: 1283–1291.
66. Hacker H, Redecke V, Blagoev B, *et al.* Specificity in Toll-like receptor signaling through distinct effector functions of TRAF3 and TRAF6. *Nature* 2006; **439**: 204–207.
67. Oganesyan G, Saha SK, Guo B, *et al.* Critical role of TRAF3 in the Toll-like receptor-dependent and –independent antiviral response. *Nature* 2006; **439**: 208–211.
68. Sasai M, Oshiumi H, Matsumoto M, *et al.* Cutting edge: NF-kappaB-activating kinase-associated protein 1 participates in TLR3/Toll-IL-1 homology domain-containing adapter molecule-1-mediated IFN regulatory factor 3 activation. *Journal of Immunology* 2005; **174**: 27–30.
69. Tatematsu M, Ishii A, Oshiumi H, *et al.* A molecular mechanism for Toll/IL-1 receptor domain-containing adaptor molecule-1-mediated IRF-3 activation. *Journal of Biological Chemistry* 2010; **285**: 20128–20136.
70. Meylan E, Burns K, Hofmann K, *et al.* RIP1 is an essential mediator of Toll-like receptor 3-induced NF-kappa B activation. *Nature Immunology* 2004; **5**: 503–507.
71. Han KJ, Su X, Xu LG, Bin LH, Zhang J, Shu HB. Mechanisms of the TRIF-induced interferon-stimulated response element and NF-kappaB activation and apoptosis pathways. *Journal of Biological Chemistry* 2004; **279**: 15652–15661.
72. Kaiser WJ, Offermann MK. Apoptosis induced by the Toll-like receptor adaptor TRIF is dependent on its receptor interacting protein homotypic interaction motif. *Journal of Immunology* 2005; **174**: 4942–4952.
73. Gohda J, Matsumura T, Inoue J. Cutting edge: TNFR-associated factor (TRAF) 6 is essential for MyD88-dependent pathway but not Toll/IL-1 receptor domain-containing adaptor-inducing IFN-β (TRIF)-dependent pathway in TLR signaling. *Journal of Immunology* 2004; **173**: 2913–2917.
74. Carty M, Goodbody R, Schroder M, Stack J, Moynagh PN, Bowie A. The human adaptor SARM negatively regulates adaptor protein TRIF-dependent Toll-like receptor signaling. *Nature Immunology* 2006; **7**: 1074–1081.
75. Kayagaki N, Phung Q, Chan S, *et al.* DUBA: a deubiquitinase that regulates type I interferon production. *Science* 2007; **318**: 1628–1632.
76. Boone DL, Turer EE, Lee EG, *et al.* The ubiquitin-modifying enzyme A20 is required for termination of Toll-like receptor responses. *Nature Immunology* 2004; **5**: 1052–1060.
77. Edelman KH, Richardson-Burns S, Alexopoulou L, Tyer KL, Flavell RA, Oldstone MBA. Does Toll-like receptor 3 play a biological role in virus infections? *Virology* 2004; **322**: 231–238.
78. Hardarson HS, Baker JS, Yang Z, *et al.* Toll-like receptor 3 is an essential component of the innate stress response in virus-induced cardiac injury. *American Journal of Physiology. Heart and Circulatory Physiology* 2007; **292**: 251–258.

Copyright © 2011 John Wiley & Sons, Ltd.

79. Abe Y, Nagata N, Sata T, Takeuchi O, Akira S, Koike S. TLR3-TRIF pathway is important for type I IFN responses in poliovirus infection. *Proceedings of 57th Annual Meeting of the Japanese Society for Virology* 2009; 234.
80. Oshiumi H, Matsumoto M, Seya T. TICAM-1/TRIF, a TLR3 adaptor, is essential for protection against poliovirus infection. *International Immunology* 2010 **22**(Suppl. 1) i19. (abstract).
81. Racaniello VR. Picornaviridae: the viruses and their replication. In *Fields Virology*, 5th edn, Knipe DM, Howly PM (eds). Lippincott Williams & Wilkins: Philadelphia, 2007; 795–838.
82. Negishi H, Osawa T, Ogami K, *et al.* A critical link between Toll-like receptor 3 and type II interferon signaling pathways in antiviral innate immunity. *Proceedings of the National Academy of Science of the United States of America* 2008; **105**: 20446–20451.
83. Wang T, Town T, Alexopoulou L, Anderson JF, Fikrig E, Flavell RA. Toll-like receptor 3 mediates West Nile virus entry into the brain causing lethal encephalitis. *Nature Medicine* 2004; **10**: 1366–1373.
84. Daffis S, Samuel MA, Suthar MS, Gale M Jr, Diamond MS. Toll-like receptor 3 has a protective role against West Nile virus infection. *Journal of Virology* 2008; **82**: 10349–10358.
85. Guillot L, Goffic RL, Bloch S, *et al.* Involvement o Toll-like receptor 3 in the immune response of lung epithelial cells to double-stranded RNA and influenza A virus. *Journal of Biological Chemistry* 2005; **280**: 5571–5580.
86. Rudd BD, Burstein E, Duckett CS, Li X, Lukacs NW. Differential role for TLR3 in respiratory syncytial virus-induced chemokine expression. *Journal of Virology* 2005; **79**: 3350–3357.
87. Rudd BD, Smit JJ, Flavell RA, *et al.* Deletion of TLR3 alters the pulmonary immune environment and mucs production during respiratory syncytial virus infection. *Journal of Immunology* 2006; **176**: 1937–1942 .
88. Goffic RL, Baalloy V, Lagranderie M, *et al.* Detrimental contribution of the Toll-like receptor (TLR) 3 to influenza A virus-induced acute pneumonia. *PLoS Pathogens* 2006; **2**: 526–535.
89. Gowen BB, Hoopes JD, Wong M-H, *et al.* TLR3 deletion limits mortality and disease severity due to phlebovirus infection. *Journal of Immunology* 2006; **177**: 6301–6307.
90. Tabeta K, Georgel P, Janssen E, *et al.* Toll-like receptor 9 and 3 as essential components of innate immune defense against mouse cytomegalovirus infection. *Proceedings of the National Academy of Science of the United States of America* 2004; **101**: 3516–3521.
91. Heath WR, Belz GT, Behrens GM, *et al.* Cross-presentation, dendritic cell subsets, and the generation of immunity to cellular antigens. *Immunology Reviews* 2004; **199**: 9–26.
92. Shen L, Lock KL. Priming of T cells by exogenous antigen cross-presented on MHC class I molecules. *Current Opinion in Immunology* 2006; **18**: 85–91.
93. Edwards AD, Diebold SS, Slack EM, *et al.* Toll-like receptor expression in murine DC subsets: lack of CD8 α+ DC correlates with unresponsiveness to imidazoquinolines. *European Journal of Immunology* 2003; **33**: 827–833.
94. Jongbloed SL, Kassianos AJ, McDonald KJ, *et al.* Human CD141+ (BDCA-3)+ dendritic cells (DCs) represent a unique myeloid DC subset that cross-presents necrotic cell antigens. *Journal of Experimental Medicine* 2010; **207**: 1247–1260.
95. Poulin LF, Salio M, Griessinger E, *et al.* Characterization of human DNGR-1+ BDCA3+ leukocytes as putative equivalents of mouse CD8α+ dendritic cells. *Journal of Experimental Medicine* 2010; **207**: 1261–1271.
96. Bachem A, Güttler S, Hartung E, *et al.* Superior antigen cross-presentation and XCR1 expression define human CD11c+ CD141+ cells as homologues of mouse CD8+ dendritic cells. *Journal of Experimental Medicine* 2010; **207**: 1273–1281.
97. Crozat K, Guiton R, Contreras V, *et al.* The XC chemokine receptor 1 is a conserved selective marker of mammalian cells homologous to mouse CD8α+ dendritic cells. *Journal of Experimental Medicine* 2010; **207**: 1283–1292.
98. Schultz O, Diebold SS, Chen M, *et al.* Toll-like receptor 3 promotes cross-priming to virus-infected cells. *Nature* 2005; **433**: 887–892.
99. Bon AL, Etchart N, Rossmann C, *et al.* Cross-priming of CD8+ T cells stimulated by virus-induced type I interferon. *Nature Immunology* 2003; **4**: 1009–1015.
100. Ebihara T, Shingai M, Matsumoto M, Wakita T, Seya T. Hepatitis C virus (HCV)-infected apoptotic cells extrinsically modulate dendritic cell function to activate T cells and NK cells. *Hepatology* 2008; **48**: 48–58.
101. Zhang S-Y, Jouanguy E, Ugolini S, *et al.* TLR3 deficiency in patients with Herpes Simplex encephalitis. *Science* 2007; **317**: 1522–1527.
102. Lauterbach H, Bathke B, Gilles S, *et al.* Mouse CD8α+ DCs and human BDCA3+ DCs are major producers of IFN-λ in response to poly(I:C). *Journal of Experimental Medicine* 2010; **207**: 2703–2717.
103. Akazawa T, Ebihara T, Okuno M, *et al.* Antitumor NK activation induced by the TLR3–TICAM-1 (TRIF) pathway in myeloid dendritic cells. *Proceedings of the National Academy of Science of the United States of America* 2007; **104**: 252–257.
104. Ebihara T, Azuma M, Oshiumi H, *et al.* Identification of a polyI:C-inducible membrane protein that participates in dendritic cell-mediated natural killer cell activation. *Journal of Experimental Medicine* 2010; **207**: 2675–2687.
105. Miyake T, Kumagai Y, Kato H, *et al.* Poly I:C-induced activation of NK cells by CD8 alpha+ dendritic cells via the IPS-1 and TRIF-dependent pathways. *Journal of Immunology* 2009; **183**: 2522–2528.
106. McCartney S, Vermi W, Gilfillan S, *et al.* Distinct and complementary functions of MDA5 and TLR3 in poly(I:C)-mediated activation of mouse NK cells. *Journal of Experimental Medicine* 2009; **206**: 2967–2976.
107. Lee HKS, Dunzendorfer K, Soldau K, Tobias PS. 2006; Double-stranded RNA-mediated TLR3 activation is enhanced by CD14. *Immunity* **24**: 153–163.
108. Kim J-I, Lee CJ, Jin MS, *et al.* Crystal structure of CD14 and its implications for lipopolysaccharide signaling. *Journal of Biological Chemistry* 2005; **280**: 11347–11351.
109. Itoh K, Watanabe A, Funami K, Seya T, Matsumoto M. The clathrin-mediated endocytic pathway participates in dsRNA-induced IFN-β production. *Journal of Immunology* 2008; **181**: 5522–5529.
110. Okahira S, Nishikawa F, Nishikawa S, Akazawa T, Seya T, Matsumoto M. Interferon-β induction through Toll-like receptor 3 depends on double-stranded RNA structure. *DNA and Cell Biology* 2005; **24**: 614–623.
111. Gowen BB, Wong M-H, Jung K-H, *et al.* TLR3 is essential for induction of protective immunity against Punta Toro virus infection by the double-stranded RNA (dsRNA), poly(I:C12U), but not poly(I:C): differential recognition of synthetic dsRNA molecules. *Journal of Immunology* 2007; **178**: 5200–5208.

Copyright © 2011 John Wiley & Sons, Ltd.

Supplemental Material can be found at:
http://www.jbc.org/content/suppl/2011/01/25/M110.185793.DC1.html

THE JOURNAL OF BIOLOGICAL CHEMISTRY VOL. 286, NO. 12, pp. 10702–10711, March 25, 2011
© 2011 by The American Society for Biochemistry and Molecular Biology, Inc. Printed in the U.S.A.

Raftlin Is Involved in the Nucleocapture Complex to Induce Poly(I:C)-mediated TLR3 Activation*[S]

Received for publication, September 15, 2010, and in revised form, January 23, 2011 Published, JBC Papers in Press, January 25, 2011, DOI 10.1074/jbc.M110.185793

Ayako Watanabe[‡], Megumi Tatematsu[‡], Kazuko Saeki[§], Sachiko Shibata[¶], Hiroaki Shime[‡], Akihiko Yoshimura[‖], Chikashi Obuse[¶], Tsukasa Seya[‡], and Misako Matsumoto[‡1]

From the [‡]Department of Microbiology and Immunology, Hokkaido University Graduate School of Medicine, Kita 15, Nishi 7, Kita-ku, Sapporo 060-8638, the [§]Department of Medical Biochemistry, Graduate School of Medical Sciences, Kyushu University, Fukuoka 812-8582, the [¶]Division of Molecular Life Science, Graduate School of Life Science, Hokkaido University, Sapporo 001-0021, and the [‖]Department of Microbiology and Immunology, School of Medicine, Keio University, Tokyo 160-8582, Japan

The double-stranded RNA analog, poly(I:C), extracellularly activates both the endosomal Toll-like receptor (TLR) 3 and the cytoplasmic RNA helicase, melanoma differentiation-associated gene 5, leading to the production of type I interferons (IFNs) and inflammatory cytokines. The mechanism by which extracellular poly(I:C) is delivered to TLR3-positive organelles and the cytoplasm remains to be elucidated. Here, we show that the cytoplasmic lipid raft protein, Raftlin, is essential for poly(I:C) cellular uptake in human myeloid dendritic cells and epithelial cells. When Raftlin was silenced, poly(I:C) failed to enter cells and induction of IFN-β production was inhibited. In addition, cellular uptake of B-type oligodeoxynucleotide that shares its uptake receptor with poly(I:C) was suppressed in Raftlin knockdown cells. Upon poly(I:C) stimulation, Raftlin was translocated from the cytoplasm to the plasma membrane where it colocalized with poly(I:C), and thereafter moved to TLR3-positive endosomes. Thus, Raftlin cooperates with the uptake receptor to mediate cell entry of poly(I:C), which is critical for activation of TLR3.

Polyriboinosinic:polyribocytidylic acid (poly(I:C)),[2] a synthetic double-stranded RNA (dsRNA), has been used as a potent type I interferon (IFN-α/β) inducer in both *in vitro* and *in vivo* studies since the discovery of anti-viral activity of type I IFNs (1–3). Many types of cells including fibroblasts, epithelial cells, and myeloid dendritic cells (DCs), produce IFN-β upon stimulation with poly(I:C). Studies have demonstrated that extracellular poly(I:C) is recognized by Toll-like receptor (TLR) 3 and cytoplasmic RNA helicase, melanoma differentiation-associated gene 5 (MDA5), and induces innate immune responses including the production of type I IFNs and inflammatory cytokines (4–8). More recently, experimental evidence has accumulated that poly(I:C) acts as an adjuvant that enhances antibody production, natural killer cell activation, and cytotoxic T lymphocyte induction through the activation of TLR3 and/or MDA5 (9–15).

Human TLR3 localizes to the endosomal compartments in myeloid DCs, whereas it localizes to both the cell surface and endosomes of fibroblasts, macrophages, and epithelial cells (5, 16, 17). TLR3 signaling arises from an intracellular compartment in both cell types and requires endosomal maturation. After dsRNA recognition, endosomal TLR3 recruits an adaptor molecule, *i.e.* Toll-IL-1 receptor domain-containing adaptor molecule-1 (TICAM-1, also called TRIF) that activates the NF-κB, IRF-3, and AP-1 transcription factors, leading to IFN-β production (18, 19). Also, extracellular poly(I:C) is sensed by MDA5 in the cytoplasm, resulting in the activation of IRF-3 and NF-κB via the mitochondrial outer membrane protein IPS-1 (also called MAVS, Cardif, or VISA) (20–23). However, the mechanism by which poly(I:C) is delivered from the extracellular fluid to the intracellular dsRNA sensors remains unresolved.

A recent study showed that CD14 directly binds to poly(I:C) and mediates poly(I:C) cellular uptake (24). Bone marrow-derived macrophages from CD14-deficient mice exhibited impaired, but not completely diminished, responses to poly(I:C). Also, a class A scavenger receptor was identified as a cell surface receptor for poly(I:C) in human epithelial cells, although the response of poly(I:C) was only partially impaired in scavenger receptor A-deficient mice (25). These results suggest that an unidentified cell surface molecule mediates cell entry of poly(I:C). Indeed, we and others demonstrated that poly(I:C) is internalized into CD14-negative human myeloid DCs and HEK293 cells via clathrin-dependent endocytosis, and B- and C-type oligodeoxynucleotides (ODNs) share the uptake receptor with poly(I:C) (26–28).

In this study, we isolated poly(I:C)-binding proteins from CD14-negative cell lysates by sequential affinity chromatography with poly(U)- and poly(I:C)-Sepharose and subjected them to mass spectrometric analysis. Among the proteins identified, we selected several proteins that exhibited a transmembrane domain or a membrane-anchoring motif and examined whether they were involved in poly(I:C)-induced TLR3-mediated signaling. We found that Raftlin, a major lipid raft protein

* This work was supported in part by grants-in-aid from the Ministry of Education, Science, and Culture, the Ministry of Health, Labor, and Welfare of Japan, and the Akiyama Foundation, NorthTec Foundation, Yakult Foundation, and the Program of Founding Research Centers for Emerging and Reemerging Infectious Diseases, MEXT.

[S] The on-line version of this article (available at http://www.jbc.org) contains supplemental Tables S1–S3 and Figs. S1–S4.

[1] To whom correspondence should be addressed. Tel.: 81-11-706-6056; Fax: 81-11-706-7866; E-mail: matumoto@pop.med.hokudai.ac.jp.

[2] The abbreviations used are: poly(I:C), polyriboinosinic:polyribocytidylic acid; 4F2, 4F2 cell-surface antigen heavy chain; DCs, dendritic cells; BMDC, bone marrow-derived DC; CTXB, cholera toxin subunit B; MDA5, melanoma differentiation-associated gene 5; MβCD, methyl-β-cyclodextrin; MoDC, monocyte-derived immature DC; ODN, oligodeoxynucleotide; TICAM-1, Toll-IL-1 receptor-containing adaptor molecule-1; TLR, Toll-like receptor.

Downloaded from www.jbc.org at HOKKAIDO DAIGAKU, on May 11, 2011

expressed by B cells, plays a critical role in poly(I:C) cellular uptake in human myeloid DCs and epithelial cells.

EXPERIMENTAL PROCEDURES

Cell Culture and Reagents—Human B cell lines Raji, BALL-1, and Namalwa were obtained from the Riken Cell Bank (Tukuba, Japan) and maintained in RPMI 1640 supplemented with 10% heat-inactivated FCS (BioSource Intl., Inc.) and antibiotics. HEK293 cells were obtained from Sumitomo Pharmaceuticals Co., Ltd. (Osaka, Japan) and maintained in Dulbecco's modified Eagle's medium low glucose (Invitrogen) supplemented with 10% heat-inactivated FCS and antibiotics. HeLa cells were kindly provided by Dr. T. Fujita (Kyoto University) and maintained in Eagle's minimal essential medium (Nissui, Tokyo, Japan) supplemented with 1% L-glutamine and 10% heat-inactivated FCS. Human monocyte-derived immature DCs (MoDCs) were generated from $CD14^+$ monocytes by culturing for 6 days in the presence of 500 units/ml of granulocyte-macrophage colony-stimulating factor and 100 units/ml of IL-4 (PeproTech). Bone marrow-derived DCs (BMDCs) were prepared as described (10). Polymyxin B, 4′,6-diamidine-2′-phenylindole dihydrochloride (DAPI), saponin, and methyl-β-cyclodextrin (MβCD) were purchased from Sigma. Poly(I:C) was from Amersham Biosciences, FITC-labeled ODN2006 was from InvivoGen, Alexa Fluor 488/cholera toxin subunit B (CTXB) and Alexa Fluor 568/transferrin were from Molecular Probes. MALP-2 was obtained from Biosynthesis (Nagoya, Japan). In addition, the following antibodies were used in this study: anti-dsRNA mAb (K1) (BioLink), anti-β actin mAb (Sigma), anti-clathrin heavy chain mAb (TD.1) (Santa Cruz Biotechnology), anti-Rab5 mAb (Abcam), anti-LAMP1 (H4A3) (BioLegend), HRP-conjugated secondary Abs (BIOSOURCE), FITC-labeled goat anti-mouse IgG (American Qualex), and Alexa Fluorp®-conjugated secondary antibodies (Invitrogen). Anti-human Raftlin polyclonal antibody was prepared as described (29). Anti-human TLR3 mAb (clone TLR3.7) was generated in our laboratory (5). Texas Red-labeled poly(I:C) was prepared using the 5′ EndTag™ Nucleic Acid Labeling System (Vector Laboratories, Burlingame, CA) according to the manufacturer's instructions.

Mice—Raftlin$^{-/-}$ mice were provided by Dr. A. Yoshimura (Keio University). Mice were maintained under specific pathogen-free conditions in the animal facility of the Hokkaido University Graduate School of Medicine. Animal experiments were performed according to the guidelines established by the Hokkaido University Animal Care and Use Committee.

Plasmids—The cDNA fragment encoding the ORF of human TLR2 or TLR3 was amplified by RT-PCR from total RNA prepared from MoDCs, and was ligated into the cloning site of the expression vector pEF-BOS, a gift from Dr. S. Nagata (Kyoto University) (5). Complementary DNA for human Raftlin was generated by PCR from cDNA derived from Raji cells using specific primers (forward primer, 5′-CTCGAGGCCGCCACCATGGGTTG-3′; reverse primer, 5′-GGATCCTTGTTTTCTTCAACCGTACCAAGCTC-3′), and was ligated into the cloning site of the expression vector pEYFP-N1 (C-terminal yellow fluorescent protein (YFP) tag, Clontech).

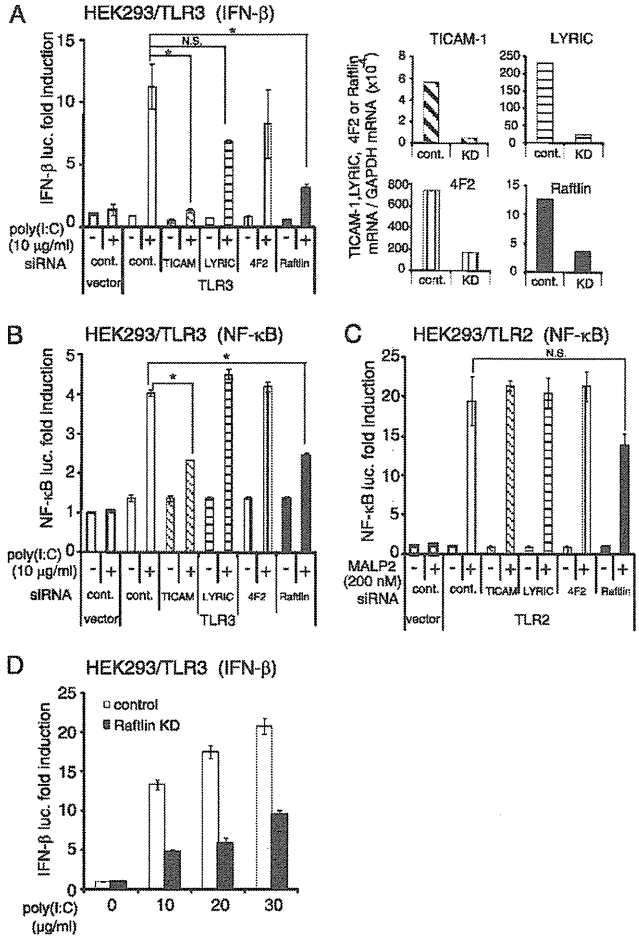

FIGURE 1. **Raftlin participates in poly(I:C)-induced TLR3-mediated signaling.** HEK293 cells were transfected with the indicated siRNAs (20 pmol) together with the expression vector for human TLR3 (*A*, *B*, and *D*), human TLR2 (*C*), or empty vector and reporter plasmid. Forty-eight hours after transfection, cells were washed and stimulated with 10–30 μg/ml of poly(I:C) or 200 nM MALP-2. After 6 h, the luciferase reporter activities were measured and expressed as fold-induction relative to the activity of unstimulated vector-transfected cells. Representative data from a minimum of three separate experiments are shown (mean ± S.D.). In each experiment, knockdown (*KD*) efficiency was assessed 48 h after transfection by qPCR. Expression of each gene was normalized to GAPDH mRNA expression. As shown in the *right-hand panels* of *A*, expression of the indicated genes is efficiently silenced (knockdown efficiency: TICAM-1, 91.4%; LYRIC, 89.5%; 4F2, 77.4%; Raftlin, 71.8%). *, $p < 0.05$ (*t* test).

Isolation of Poly(I:C)-binding Proteins—Raji cells (1×10^{10}) were washed twice with Dulbecco's phosphate-buffered saline, frozen and thawed three times in Dulbecco's phosphate-buffered saline (5×10^7/ml), and centrifuged at 20,000 × *g* for 10 min. Cell pellets were lysed in lysis buffer (1% Nonidet P-40 in buffer A (20 mM Tris-HCl, pH 7.4, 140 mM NaCl, 25 mM iodoacetamide, 10 mM EDTA, 2 mM PMSF and protease inhibitor mixture)) for 20 min at room temperature. After centrifugation at 10,000 × *g* for 10 min, supernatants were filtrated with Minisalt GF (Zartorius stedim, Japan) and sequentially applied to Sepharose, poly(U)-Sepharose, and poly(I:C)-Sepharose equilibrated with binding buffer (0.2% Nonidet P-40 in buffer A). The poly(I:C)-binding molecules were eluted from poly(I:C)-Sepharose with elution buffer (1.4 M NaCl in washing buffer) after being washed with washing buffer (10 mM CHAPS in buffer A). The eluates were

Downloaded from www.jbc.org at HOKKAIDO DAIGAKU, on May 11, 2011

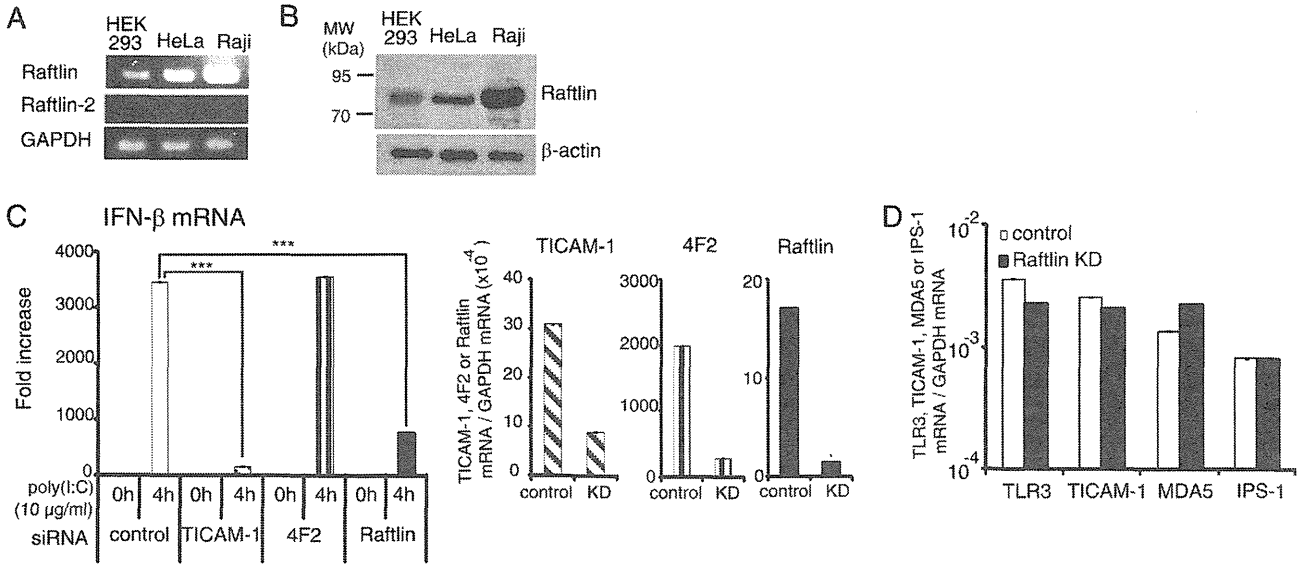

FIGURE 2. **Raftlin is essential for poly(I:C)-induced IFN-β production in HeLa cells.** *A*, expression of Raftlin and Raftlin-2 mRNAs in human cell lines. *B*, protein expression level of Raftlin in human cell lines. Cell lysates (3 μg) were separated on 10% SDS-PAGE, followed by immunoblotting with anti-Raftlin pAb or anti-β-actin mAb. *C*, poly(I:C)-induced IFN-β mRNA expression in HeLa cells. HeLa cells were transfected with the indicated siRNAs (20 pmol) using Lipofectamine 2000. Forty-eight hours after transfection, cells were washed and stimulated with 10 μg/ml of poly(I:C) for 4 h (*left-hand panel*). Total RNA was extracted and qPCR was performed using primers for the respective genes (*C* and *D*). Expression of each gene was normalized to GAPDH mRNA expression. Data are shown as the mean ± S.D., although the values are too small to represent. Representative data from three independent experiments are shown. ***, $p < 0.001$.

mixed with new poly(U)-Sepharose and rotated for 1 h at 4 °C. After centrifugation, supernatants were mixed with new poly(I:C)-Sepharose. The poly(U)- and poly(I:C)-Sepharose were washed three times with 5 volumes of washing buffer and binding molecules were eluted with elution buffer. The eluates were concentrated using YM-50 Microcon (Millipore).

Mass Spectrometry—The poly(U)- or poly(I:C)-binding molecules were separated on a 10% SDS-PAGE gel under reducing conditions, and the region of the gels containing proteins from about 250,000 to 20,000 was cut at about 1–2-mm intervals as described previously (30). After in-gel digestion with modified trypsin, the resulting peptides were analyzed by LC/MS/MS. The ion spectrum data generated by LC/MS/MS were screened against the international protein index human data base (version 3.29) with Mascot (Matrix Science, London, UK) to identify high-scoring proteins.

RNA Interference and Luciferase Reporter Assay—siRNA duplexes (LYRIC, catalog number s40866; 4F2, catalog number s12944; Raftlin, catalog numbers s23219, s23217, and s23218; negative control, catalog number AM4635) were obtained from Ambion-Applied Biosystems. siRNA for TICAM-1 was purchased from Xeragon Inc. (Birmingham, AL) (18). HEK293 cells cultured in 24-well plates were transfected with 20 pmol of each siRNA together with the expression vector for human TLR3 or TLR2 (200 ng), IFN-β promoter or ELAM reporter plasmid (60 ng), and an internal control vector (1.5 ng) using Lipofectamine 2000. Forty-eight hours after transfection, cells were washed once and then stimulated with 10 μg/ml of poly(I:C) or MALP-2 (200 nM) for 6 h. Cells were lysed and dual luciferase activities were measured according to the manufacturer's instructions (Promega). The *Firefly* luciferase activity was normalized to the *Renilla* activity and expressed as the fold-induction relative to the activity of unstimulated vector-transfected cells. In the case of HeLa cells, cells in 24-well plates were transfected with 20 pmol of each siRNA using Lipofectamine 2000. Knockdown of Raftlin in human MoDCs was preformed by electroporation as described previously (31). Briefly, MoDCs (1.4×10^6/80 μl) were transfected with control siRNA or siRNA for Raftlin (500 pmol) using a Gene-Pulser (Bio-Rad) and then cultured for 36 h in the presence of 500 milliunits/ml of granulocyte-macrophage colony-stimulating factor. The viability of the cells transfected with control and Raftlin siRNAs was 84 and 87%, respectively. Knockdown of mouse Raftlin-2 in Raftlin$^{-/-}$ BMDCs was performed with shRNA lentiviral particles (Santa Cruz) according to the manufacturer's instructions. Briefly, Raftlin$^{-/-}$ BMDCs in 24-well plates were infected with control shRNA lentiviral particles or mouse Raftlin-2 shRNA lentiviral particles at a multiplicity of infection of 2 and incubated in complete medium containing Polybrene (5 μg/ml). Twenty-four hours after infection, medium was replaced with complete medium and cells were further incubated for 24 h. The viability of the cells infected with control lentivirus and mouse Raftlin-2 shRNA-expressing lentivirus was 82 and 76%, respectively.

Quantitative PCR (qPCR)—Total RNA was extracted with the RNeasy mini kit (Qiagen, Valencia, CA) and 0.5 μg of RNA was reverse-transcribed using the high capacity cDNA Reverse Transcripition kit (Applied Biosystems) with random primers according to the manufacturer's instructions. Quantitative PCR was performed with the indicated primers (supplemental Table S1) using the Step One Real-time PCR system (Applied Biosystems).

Immunoblotting—Cells were lysed in lysis buffer (20 mM Tris-HCl, pH 7.4) containing 150 mM NaCl, 1% Nonidet P-40,

Downloaded from www.jbc.org at HOKKAIDO DAIGAKU, on May 11, 2011

10 mM EDTA, 25 mM iodoacetamide, 2 mM PMSF and a protease inhibitor mixture (Roche Applied Science). Lysates were clarified by centrifugation and subjected to SDS-PAGE (10% gel) under reducing conditions, followed by immunoblotting with anti-Raftlin pAb or anti-β actin mAb.

Immunoprecipitation—HeLa cells were stimulated with 40 μg/ml of poly(I:C) for 30 min at 37 °C. At timed intervals, cells were lysed in lysis buffer for 30 min on ice. Lysates were precleared with protein G-Sepharose (GE Healthcare) and incubated with 1 μg of anti-clathrin heavy chain mAb. Immunocomplexes were recovered by incubation with Protein G-Sepharose, washed once with lysis buffer, and resuspended in denaturing buffer. Samples were analyzed by SDS-PAGE (10% gel) under reducing conditions, followed by immunoblotting with anti-Raftlin pAb (1:1000) and HRP-conjugated secondary Ab. The membrane was re-probed with anti-clathrin heavy chain mAb (1:400).

Confocal Microscopy—HeLa cells (1×10^5 cells/well) were plated onto micro coverglasses (Matsunami Glass) in 12-well plates. The next day, cells were incubated with 40 μg/ml of poly(I:C) for 30 min at 4 °C. Cells were washed once and further incubated for 5–30 min at 37 °C. At timed intervals, cells were fixed with 4% paraformaldehyde for 30 min and permeabilized with PBS containing 0.5% saponin and 1% BSA for 30 min. Fixed cells were blocked in PBS containing 1% BSA and labeled with anti-Raftlin pAb (1:500), anti-human TLR3 mAb (20 μg/ml), or Alexa Fluor 488-CTXB (10 μg/ml) for 60 min at room temperature. Alexa Fluor 488- or Alexa Fluor 568-conjugated secondary Abs (1:400) were used to visualize the primary Abs. Nuclei were stained with DAPI (2 μg/ml) in PBS for 10 min before mounting onto glass slides using PBS containing 2.3% DABCO and 50% glycerol. Cells were visualized at a ×63 magnification with an LSM510 META microscope (Zeiss, Jena, Germany).

For uptake study, HeLa cells or HEK293 cells transfected with control siRNA or siRNA for Raftlin were incubated with 40 μg/ml of Texas Red/poly(I:C), Alexa Fluor 568/transferrin (25 μg/ml), or FITC/ODN2006 (40 μg/ml) for 30 min at 4 °C. After washing, cells were further incubated at 37 °C. At timed intervals, fixed cells were visualized as described above. In the case of HEK293 cells, cells (1×10^5 cells/well) were plated onto poly-L-lysine-coated glass (BD Bioscience) in a 24-well plate and cultured for 12 h.

Control or Raftlin knockdown MoDCs (2×10^5/100 μl) were incubated with 40 μg/ml of Texas Red/poly(I:C) for 30 min at 4 °C, washed once, and then incubated for 5–30 min at 37 °C. At timed intervals, cells were fixed with 4% paraformaldehyde for 15 min and centrifuged by Cytospin3 (Shandon). After mounting with ProLong Gold with DAPI (Molecular Probes), cells were visualized by confocal microscopy. In some experiments, MoDCs were pretreated with 1 mM MβCD for 1 h at 37 °C. Viability of cells treated with MβCD was 93.3%. For staining of endosomes, fixed cells were permeabilized with PBS containing 0.5% saponin and 1% BSA for 30 min (staining of TLR3 and early endosome), or PBS containing 100 μg/ml of digitonin and 1% BSA for 30 min (staining of late endosome). After blocking, cells were labeled with anti-Raftlin pAb (1:500), anti-human TLR3 mAb (20 μg/ml), anti-Rab5 mAb (4 μg/ml), or anti-LAMP1 mAb (H4A3) (1:200) for 60 min at room temperature.

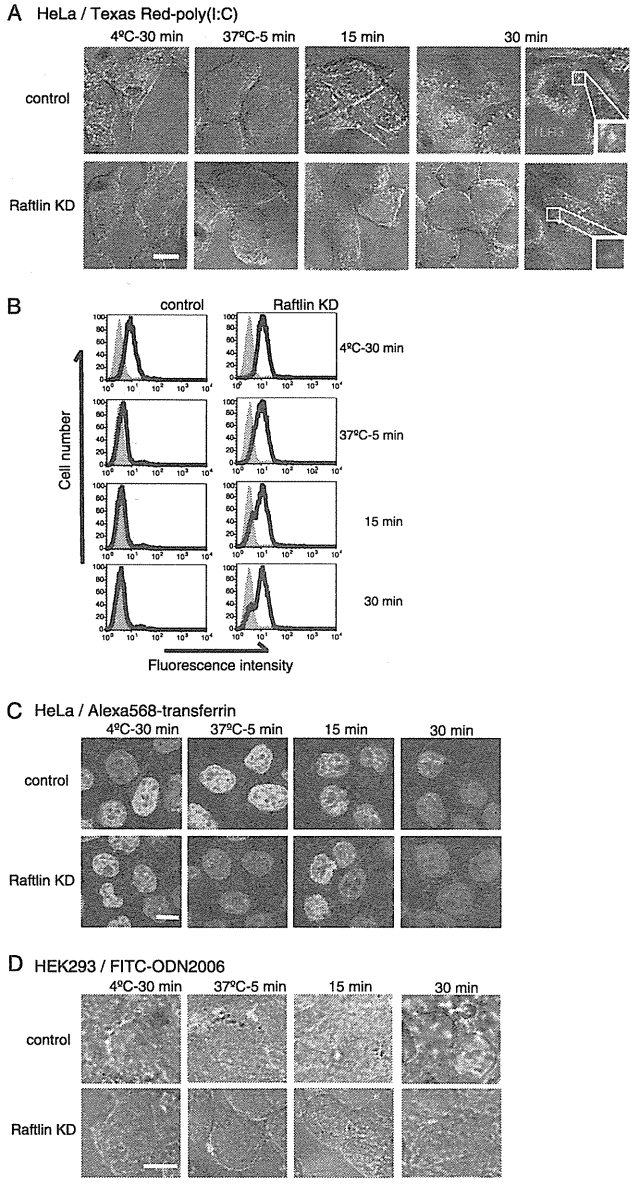

FIGURE 3. **Knockdown of Raftlin suppresses cellular uptake of poly(I:C) and B-type ODN but not transferrin.** HeLa cells (*A* and *C*) and HEK293 cells (*D*) were transfected with control siRNA (*upper panels*) or siRNA for Raftlin (*lower panels*). Forty-eight hours after transfection, cells were washed and incubated with 40 μg/ml of Texas Red/poly(I:C) (*A*), 25 μg/ml Alexa Fluor 568/transferrin (*C*), or 40 μg/ml of FITC/ODN2006 (*D*) for 30 min at 4 °C. After washing, cells were incubated for up to 30 min at 37 °C. At timed intervals, cells were fixed and visualized by confocal microscopy. In some experiments, cells were fixed or permeabilized and stained with anti-TLR3 mAb. *A*, *red*, Texas Red-poly(I:C); *green*, TLR3. *C*, *red*, Alexa 568/transferrin; *blue*, nuclei with DAPI. *D*, *green*, FITC/ODN2006. *Bar*, 10 μm. *B*, flow cytometric analysis of poly(I:C) uptake. Control and Raftlin knockdown HeLa cells were incubated with 20 μg/ml of poly(I:C) for 30 min at 4 °C. After washing, cells were incubated for up to 30 min at 37 °C. At the indicated time points, cells were labeled with anti-dsRNA mAb (*black lines*) or mouse IgG2a (*shaded histogram*) and FITC-labeled secondary Ab. The cells were analyzed on a FACS Calibur.

Flow Cytometry—Cells were incubated with the indicated concentrations of poly(I:C) in culture medium for 30 min at 4 °C. After washing, cells were labeled with anti-dsRNA mAb

Downloaded from www.jbc.org at HOKKAIDO DAIGAKU, on May 11, 2011

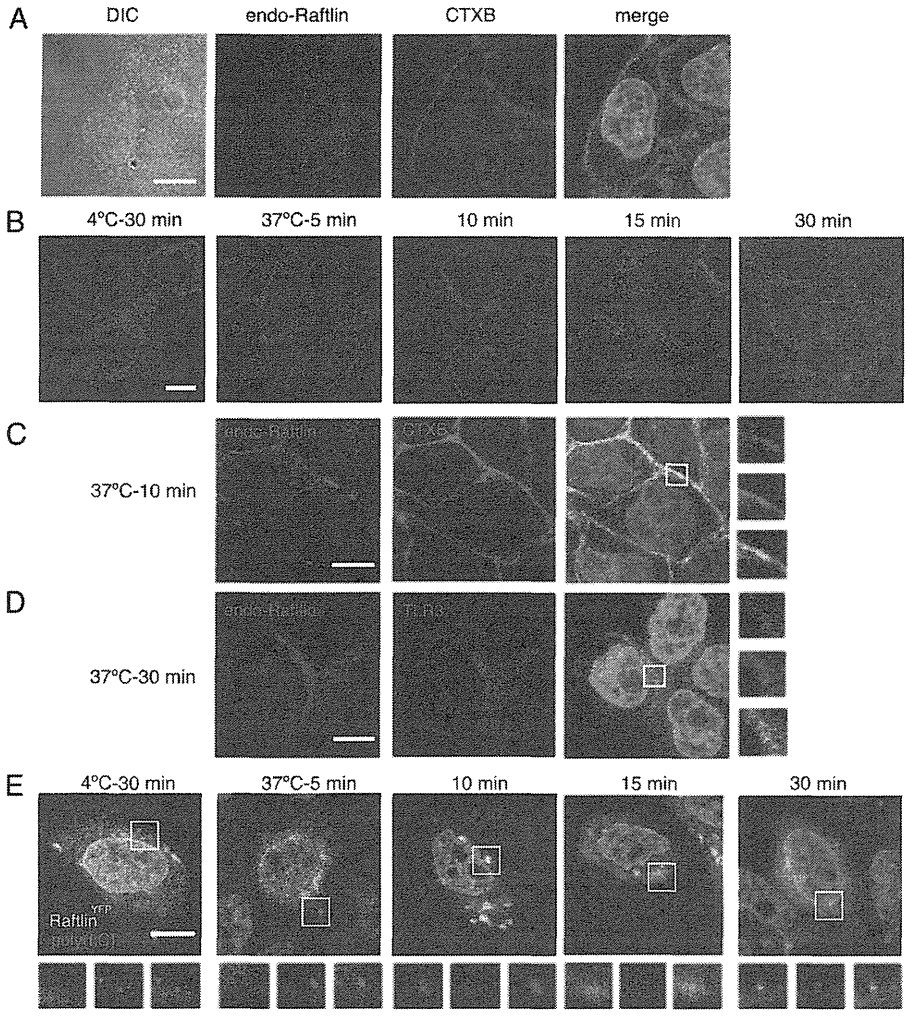

FIGURE 4. **Translocation of Raftlin in response to poly(I:C).** *A*, confocal images of endogenous Raftlin in HeLa cells. Fixed and permeabilized cells were stained with anti-Raftlin pAb and Alexa Fluor 488/CTXB. *Red*, endogenous Raftlin; *green*, CTXB; *blue*, nuclei with DAPI. *Bar*, 10 μm. *B–D*, spatiotemporal mobilization of endogenous Raftlin in response to poly(I:C). HeLa cells were incubated with 40 μg/ml of poly(I:C) as described in the legend to Fig. 3. At the indicated periods, cells were fixed and stained with anti-Raftlin pAb (*B*), anti-Raftlin pAb and Alexa Fluor 488/CTXB (*C*), or anti-Raftlin pAb and anti-TLR3 mAb (*D*). Representative data from the indicated time points are shown. *B* and *C*, *red*, endogenous Raftlin; *green*, Alexa 488/CTXB. *D*, *green*, endogenous Raftlin; red, TLR3; *blue*, nuclei with DAPI. *Bar*, 10 μm. *E*, association of Raftlin with poly(I:C). Confocal images of poly(I:C) uptake by HeLa cells expressing Raftlin^{YFP}. HeLa cells were transfected with Raftlin^{YFP} and incubated with 40 μg/ml of Texas Red/poly(I:C) as described above. At the indicated periods, cells were fixed and visualized by confocal microscopy. *Lower panels* show ×2 magnified images of the *insets* in the *upper panels*. *Yellow*, Raftlin^{YFP}; *red*, Texas Red/poly(I:C); *blue*, nuclei with DAPI. *Bar*, 10 μm.

(K1) or mouse IgG2a as a control (1 μg) in the presence of human IgG (10 μg) for 30 min at 4 °C in FACS buffer (Dulbecco's phosphate-buffered saline containing 0.5% BSA and 0.1% sodium azide) and then incubated with FITC-labeled secondary Ab. Cells were analyzed on a FACS Calibur flow cytometer (BD Biosciences).

Statistical Analysis—Statistical significance of differences between groups was determined by the Student's *t* test.

RESULTS

Raftlin Participates in Poly(I:C)-induced TLR3-mediated Signaling—We previously demonstrated that poly(I:C) binds to human MoDCs and HEK293 cells (27). Because poly(I:C) also activates B cells (32), we screened B cell lines capable of binding poly(I:C) and found that Raji cells bound poly(I:C) at an equivalent level to MoDCs (supplemental Fig. S1). To identify the proteins involved in poly(I:C) cellular uptake, we isolated the poly(I:C)-binding proteins from Raji cell lysates by sequential affinity chromatography using Sepharose, poly(U)-Sepharose, and poly(I:C)-Sepharose. The eluate from poly(U)- or poly(I:C)-Sepharose was subjected to SDS-PAGE, followed by mass spectrometric analyses. A total of 127 proteins were identified, which preferentially bound to poly(I:C)-Sepharose rather than to poly(U)-Sepharose (supplemental Table S2). They included several proteins with a dsRNA-binding motif, such as interferon-induced dsRNA-activated protein kinase (supplemental Table 3). Also, clathrin heavy chain 1 and several cytoskeleton molecules, such as tubulin and actinin-1, were identified, suggesting that poly(I:C) uptake machinery might be isolated from the cell lysates as a complex. In the membrane/cytoskeleton group, only four are membrane-associated proteins (supplemental Table S3). We selected transmembrane proteins LYRIC

Downloaded from www.jbc.org at HOKKAIDO DAIGAKU, on May 11, 2011

(also called Astrocyte elevated gene 1) and 4F2 cell surface antigen heavy chain (4F2, also named CD98), and a cytoplasmic protein Raftlin that contains a membrane-anchoring motif at the N terminus. Because HEK293 cells express these molecules, we first examined whether they are involved in poly(I:C)-induced TLR3-mediated signaling by gene silencing. As a positive control, knockdown of TICAM-1 was performed. Interestingly, poly(I:C)-induced TLR3-mediated IFN-β promoter activation was greatly reduced when Raftlin was knocked down in HEK293 cells, whereas silencing of the LYRIC or 4F2 genes did not affect poly(I:C) function (Fig. 1*A*, *left-hand panel*). Poly(I:C)-induced TLR3-mediated NF-κB activation was also decreased in Raftlin knockdown HEK293 cells, in a similar way to TICAM-1 knockdown cells (Fig. 1*B*). In contrast, TLR2-mediated NF-κB activation was substantially induced in all cells subjected to gene silencing (Fig. 1*C*). The failure of IFN-β promoter activation in Raftlin knockdown HEK293 cells was also observed when cells were stimulated with increasing amounts of poly(I:C) (Fig. 1*D*). These results strongly suggest that Raftlin participates in poly(I:C)-induced TLR3 activation.

Raftlin Is Essential for Poly(I:C)-induced IFN-β Production in HeLa Cells—Raftlin was originally identified as a major lipid raft protein required for lipid raft integrity, B cell receptor signal transduction, and modulation of T cell receptor signaling (29, 33). We analyzed the expression of Raftlin and Raftlin-2, a homologue of Raftlin, in HEK293, HeLa, and Raji cells by RT-PCR. As shown in Fig. 2*A*, these cell lines express Raftlin but not Raftlin-2 mRNA. The protein expression level of Raftlin was further examined by immunoblotting with an anti-human Raftlin pAb (29). Raftlin was abundantly expressed in Raji cells, and expressed at lower levels in HEK293 and HeLa cells (Fig. 2*B*). Poly(I:C)-induced IFN-β mRNA expression was greatly diminished by knockdown of Raftlin in HeLa cells, in a similar way to TICAM-1 knockdown. In contrast, HeLa cells transfected with siRNA for 4F2 or LYRIC efficiently responded to poly(I:C) (Fig. 2*C*, *left-hand panel*, and supplemental Fig. S2). The expression of TLR3, TICAM-1, MDA5, and IPS-1 was not affected by knockdown of Raftlin (Fig. 2*D*). Thus, Raftlin plays a critical role in poly(I:C)-induced IFN-β production.

Raftlin Is Indispensable for Poly(I:C) Cellular Uptake—To examine the role of Raftlin in poly(I:C)-induced cellular responses, we analyzed cell entry of poly(I:C) in Raftlin knockdown HeLa cells. Texas Red-labeled poly(I:C), whose biological activity was similar to that of unlabeled poly(I:C) (supplemental Fig. S3), unevenly bound to the cell surface of HeLa cells either transfected with control siRNA or Raftlin siRNA after 30 min incubation at 4 °C (Fig. 3*A*, *left panels*). When the incubation condition was changed to 37 °C for 5 min, poly(I:C) was detected as speckles at the cell surface in both cells, although some of the poly(I:C) was internalized in control cells (*second set of panels*). However, after 15 min, poly(I:C) localized diffusely in the endosomal compartments in control cells, whereas it still resided on the cell surface as speckles in Raftlin knockdown cells (*third set of panels*). Thus, clustering of the uptake receptor occurs without internalization in Raftlin knockdown cells. After 30 min, poly(I:C) accumulated in the endosomal compartments in control cells, where it colocalized with TLR3 (Fig. 3*A*, *upper right panel*). In contrast, Raftlin knockdown

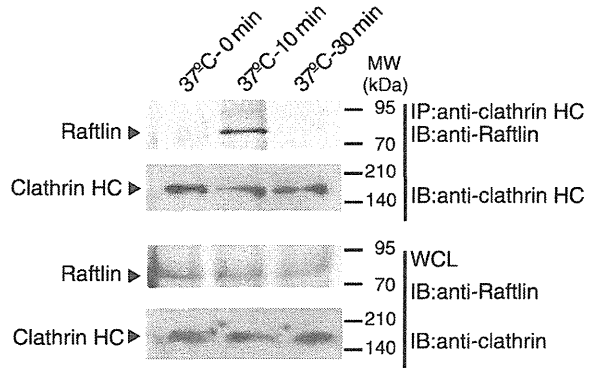

FIGURE 5. **Raftlin associates with clathrin in response to poly(I:C).** HeLa cells were stimulated with 40 μg/ml of poly(I:C) for 0–30 min at 37 °C. At timed intervals, cells were lysed in lysis buffer and clathrin was immunoprecipitated (*IP*) using an anti-clathrin heavy chain (*HC*) mAb. The immunoprecipitants were resolved on SDS-PAGE (10% gel) under reducing conditions followed by immunoblotting (*IB*) with anti-Raftlin pAb or anti-clathrin HC mAb. Whole cell lysates (*WCL*) were subjected to immunoblotting with anti-Raftlin pAb or anti-clathrin HC mAb to detect endogenous protein expression. Molecular mass markers are indicated on the *right*.

HeLa cells did not permit cell entry of poly(I:C). Consistent with these results, flow cytometric analysis showed that surface poly(I:C) disappeared in control but not in Raftlin knockdown HeLa cells (Fig. 3*B*). After a 30-min incubation at 37 °C, poly(I:C) was detected on the cell surface of ~80% of HeLa cells transfected with Raftlin-siRNA, which reflects the knockdown efficiency.

Because poly(I:C) is internalized into cells by the clathrin-dependent endocytic pathway, we examined whether uptake of transferrin, which occurs in a clathrin-dependent manner, is suppressed by Raftlin knockdown. As shown in Fig. 3*C*, transferrin was internalized into HeLa cells irrespective of Raftlin knockdown. We previously reported that B- and C-type ODNs share their uptake receptor with poly(I:C) in HEK293 cells and MoDCs and are delivered to TLR3-positive endosomes in MoDCs (27). Indeed, FITC-labeled B-type ODN (ODN 2006) failed to enter cells when Raftlin was silenced in HEK293 cells (Fig. 3*D*). These results indicate that Raftlin is essential for uptake of poly(I:C) and B- and C-type ODNs via receptor-mediated endocytosis.

Raftlin Is Involved in the Uptake Machinery for Poly(I:C)—A previous study showed that Raftlin is localized exclusively in lipid rafts by fatty acylation of the N-terminal Gly-2 and Cys-3 residues in human B cells (29). We analyzed the subcellular localization of Raftlin in HeLa cells. Endogenous Raftlin was localized diffusely in the cytoplasm and did not merge with CTXB, which binds to the lipid raft molecule GM1, suggesting the cell type-dependent localization of Raftlin (Fig. 4*A*). We next examined the translocation of Raftlin in response to poly(I:C). At the poly(I:C) binding step (4 °C, 30 min), Raftlin resided in the cytoplasm (Fig. 4*B*, *left panel*). After a 5-min incubation at 37 °C, most of the Raftlin remained localized in the cytoplasm. However, after 10 min, membrane-associated Raftlin was observed, which partially colocalized with CTXB (Fig. 4, *B*, *third panel*, and *C*). Interestingly, Raftlin transferred to the endosomal structures from the plasma membrane within 15 min, and colocalized with TLR3 after 30 min of incubation (Fig. 4*D*).

Downloaded from www.jbc.org at HOKKAIDO DAIGAKU, on May 11, 2011

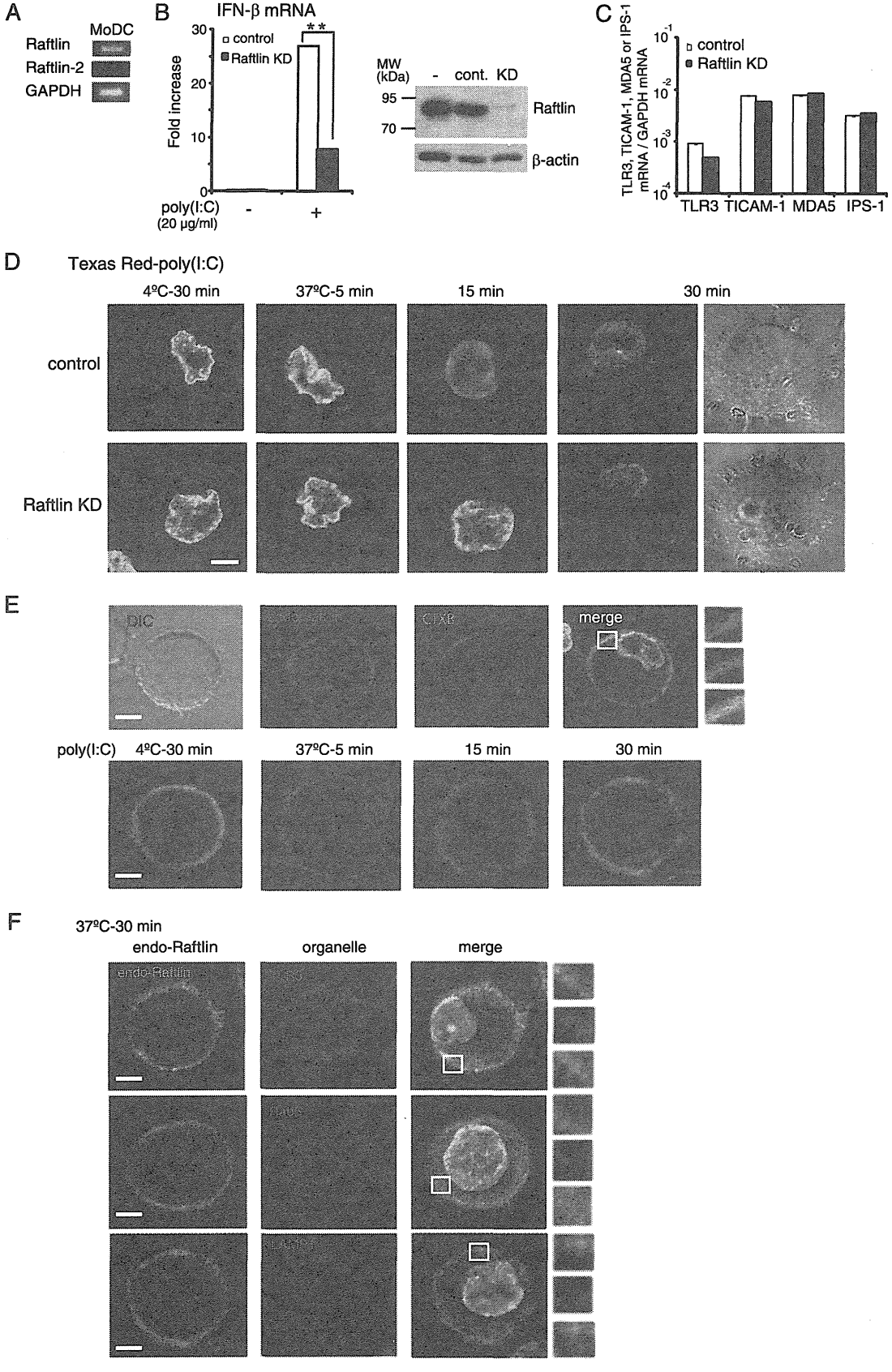

Downloaded from www.jbc.org at HOKKAIDO DAIGAKU, on May 11, 2011

To visualize the spatiotemporal mobilization of Raftlin and poly(I:C), HeLa cells were transfected with the expression vector for Raftlin^{YFP} and incubated with Texas Red-labeled poly(I:C). The subcellular localization and translocation of Raftlin^{YFP} in response to poly(I:C) were almost similar to those observed with endogenous Raftlin (Fig. 4*E*). Notably, Raftlin^{YFP} co-localized with Texas Red-poly(I:C) at the plasma membrane after 10-min incubation at 37 °C. Thereafter, poly(I:C) was internalized, spread to the endosomal compartments, and then accumulated in the organelles as shown in Fig. 3*A*. A membrane-associated Raftlin^{YFP} appeared to move along with internalized poly(I:C) (Fig. 4*E*).

To clarify the function of Raftlin in poly(I:C) internalization mediated by clathrin, we examined physical association of Raftlin with clathrin. As shown in Fig. 5, Raftlin did not interact with clathrin in unstimulated HeLa cells. When cells were stimulated with poly(I:C), Raftlin was co-immunoprecipitated with clathrin after a 10-min stimulation. However, after 30 min, Raftlin did not interact with clathrin any more. These results suggest that after poly(I:C) binding to the uptake receptor, Raftlin was recruited to the plasma membrane and associates with the clathrin complex to modulate cargo sorting and delivery.

Raftlin Is Critical for Poly(I:C)-induced IFN-β Production in Human Myeloid DCs—Human MoDCs expressed Raftlin but not Raftlin-2 mRNA (Fig. 6*A*). When DCs were electrically transfected with siRNA for Raftlin, Raftlin expression was decreased compared with cells transfected with control siRNA (Fig. 6*B*, *right-hand panel*). Poly(I:C)-induced IFN-β mRNA expression was diminished in the Raftlin knockdown DCs (Fig. 6*B*, *left-hand panel*). The mRNA expression levels of TICAM-1, MDA5, and IPS-1 in Raftlin knockdown DCs were comparable with those in control DCs, although TLR3 expression was slightly reduced compared with control cells (Fig. 6*C*). Again, entry of poly(I:C) into Raftlin knockdown DCs was inhibited (Fig. 6*D*).

Raftlin was localized to both the plasma membrane and the cytoplasm of DCs (Fig. 6*E*, *upper panels*). Although membrane-associated Raftlin partially colocalized with CTXB, lipid raft disruption with MβCD in DCs did not affect poly(I:C) cellular uptake (supplemental Fig. S4). The mobilization of Raftlin in response to poly(I:C) was similar to that observed in HeLa cells (Fig. 6*E*, *lower panels*). After 30 min, Raftlin colocalized with TLR3 and Rab5 but not with LAMP1, indicating that Raftlin, together with the poly(I:C) uptake receptor, moves from the plasma membrane to the TLR3-positive early endosomes (Fig. 6*F*).

To determine the physiological function of Raftlin, we analyzed poly(I:C)-induced IFN-β production by BMDCs from wild-type or Raftlin$^{-/-}$ mice. Remarkably, wild-type and Raftlin$^{-/-}$ BMDCs expressed mouse Raftlin-2 mRNA at equivalent levels (Fig. 7*A*). There was no significant difference in poly(I:C)-induced IFN-β production between wild-type and Raftlin$^{-/-}$ BMDCs (Fig. 7*B*). In addition, cellular uptake of poly(I:C) in Raftlin$^{-/-}$ BMDCs was comparable with that in wild-type BMDCs (Fig. 7*C*). To test the possibility that the Raftlin function is compensated with Raftlin-2 in Raftlin$^{-/-}$ BMDCs as observed in B cell receptor signaling in Raftlin$^{-/-}$ mouse B cells (33), we knocked down of mouse Raftlin-2 in Raftlin$^{-/-}$ BMDCs by infection with Raftlin-2 shRNA-expressing lentiviral particles and analyzed the cellular response to poly(I:C). Mouse Raftlin-2 expression was partially decreased in Raftlin$^{-/-}$ BMDCs (Fig. 7*D*, *right-hand panel*). Poly(I:C)-induced IFN-β mRNA expression was partially but significantly decreased in Raftlin-2 knockdown Raftlin$^{-/-}$ BMDCs (Fig. 7*D*, *left-hand panel*). Furthermore, internalization of Texas Red-labeled poly(I:C) was inhibited in ~40% of Raftlin$^{-/-}$ BMDCs infected with mouse Raftlin-2 shRNA lentiviral particles, reflecting the knockdown efficiency of mouse Raftlin-2 (Fig. 7*E*). These results suggest that mouse Raftlin-2 participates in poly(I:C) cellular uptake in Raftlin$^{-/-}$ BMDCs.

DISCUSSION

Recent studies using mouse implanted tumor models indicate that poly(I:C) is a promising adjuvant for tumor vaccines because it promotes adaptive anti-tumor responses through the activation of myeloid DCs and induction of type I IFN production by multiple type of cells (10–15). However, it remains unresolved how poly(I:C) is delivered from the extracellular fluid to the intracellular poly(I:C) sensors localized on the endosomal membrane or cytoplasm.

In this study, we demonstrated that Raftlin is essential for poly(I:C)-induced cellular responses in human myeloid DCs and epithelial cells by mediating the cellular uptake of poly(I:C). Raftlin was originally identified as a major raft protein in B cells that co-localized with B cell receptor in the lipid raft before and after B cell receptor stimulation (29). However, subcellular localization of endogenous Raftlin appears to depend on the cell types. We found that in unstimulated HeLa cells, endogenous Raftlin localized diffusely in the cytoplasm and did not co-

FIGURE 6. **Raftlin is critical for poly(I:C)-induced IFN-β production in human myeloid DCs.** *A*, MoDCs express Raftlin but not Raftlin-2 mRNA. *B*, poly(I:C)-induced IFN-β production was decreased in Raftlin knockdown DCs (*left-hand panel*). Control and Raftlin knockdown DCs in a 24-well plate (7×10^5/ml) were stimulated with 20 μg/ml of polymyxin B-treated poly(I:C) for 4 h. Total RNA was extracted and subjected to RT qPCR analysis for the expression of IFN-β. Data are representative of three separate experiments with similar results (mean ± S.D.). **, $p < 0.01$. Protein expression of Raftlin in DCs (4×10^5) before and after siRNA transfection is shown (*B*, *right panel*). *C*, expression of TLR3, TICAM-1, MDA5, and IPS-1 in DCs. Total RNA from control and Raftlin knockdown DCs were extracted and subjected to RT-qPCR analysis for the expression of mRNA. Expression of each gene was normalized to GAPDH mRNA expression. *D*, uptake of Texas Red/poly(I:C) by MoDCs transfected with control siRNA (*upper panels*) or siRNA for Raftlin (*lower panels*). Control or Raftlin knockdown DCs were incubated with 40 μg/ml of Texas Red/poly(I:C) for 30 min at 4 °C. After washing, cells were incubated for up to 30 min at 37 °C. At the indicated periods, cells were fixed and visualized by confocal microscopy. Representative images from 20 fields in the indicated time points are shown. *Red*, Texas Red/poly(I:C); *blue*, nuclei with DAPI. *Bar*, 5 μm. *E* and *F*, confocal images of endogenous Raftlin in MoDCs in response to poly(I:C). *E*, *upper panels*, DCs were fixed and stained with anti-Raftlin pAb and Alexa 488/CTXB. *Red*, endogenous Raftlin; *green*, Alexa 488/CTXB; *blue*, nuclei with DAPI. *E*, *lower panels*, and *F*, DCs were incubated with 40 μg/ml of poly(I:C) as described in the legend to Fig. 4. At the indicated periods, cells were fixed and stained with anti-Raftlin pAb, anti-TLR3 mAb, anti-Rab5 mAb, or anti-LAMP1 mAb and Alexa Fluor-conjugated secondary Abs. Representative data from the indicated time points are shown. *Green*, endogenous Raftlin; *red*, TLR3, Rab5, or LAMP-1; *blue*, nuclei with DAPI. *Bar*, 5 μm.

Downloaded from www.jbc.org at HOKKAIDO DAIGAKU, on May 11, 2011

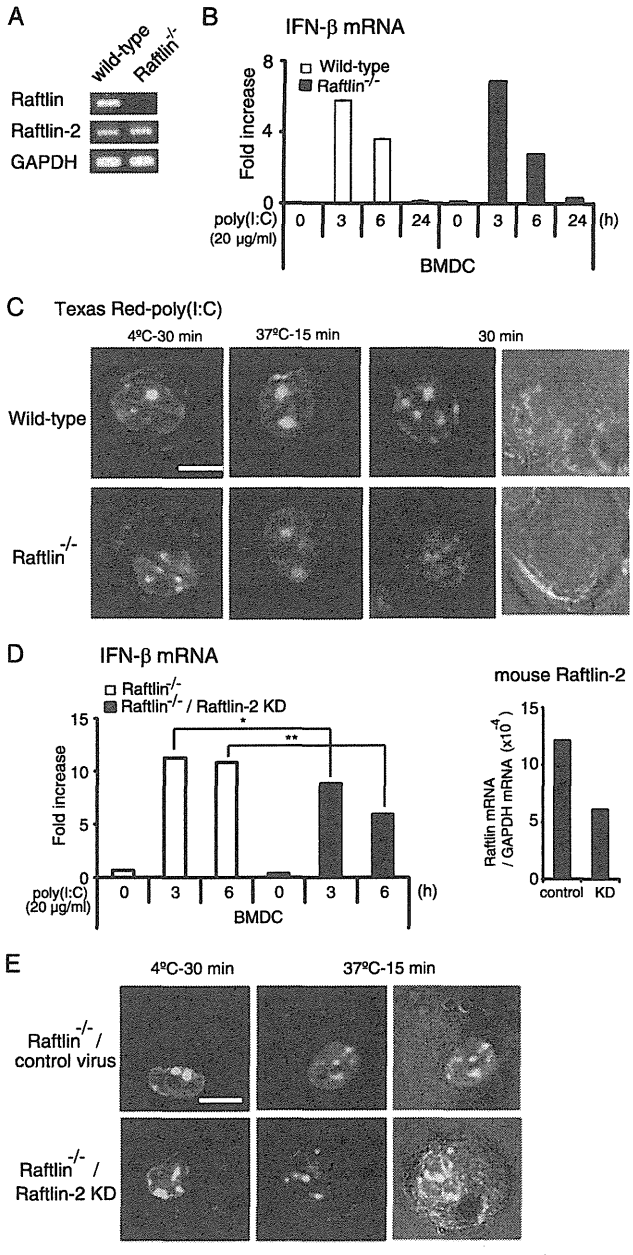

FIGURE 7. **Poly(I:C) uptake and IFN-β production by Raftlin$^{-/-}$ BMDCs.** *A*, expression of Raftlin and Raftlin-2 mRNAs in BMDCs from wild-type or Raftlin$^{-/-}$ mice. *B*, IFN-β mRNA expression in BMDCs from wild-type or Raftlin$^{-/-}$ mice in response to poly(I:C). Cells were stimulated with 20 μg/ml of polymyxin B-treated poly(I:C). At the indicated time points, cells were washed and total RNA was extracted. RT qPCR was performed using the primers for mouse IFN-β. Data (mean ± S.D.) are representative of three separate experiments with similar results. *C*, BMDCs from wild-type (*upper panels*) or Raftlin$^{-/-}$ mice (*lower panels*) were incubated with 40 μg/ml of Texas Red/poly(I:C) for 30 min at 4 °C. After washing, cells were incubated for up to 30 min at 37 °C. At timed intervals, cells were fixed and visualized by confocal microscopy. Representative images from 20 fields in the indicated time points are shown. *Red*, Texas Red/poly(I:C); *blue*, nuclei with DAPI. *Bar*, 5 μm. *D*, poly(I:C)-induced IFN-β mRNA expression in control and Raftlin-2 knockdown Raftlin$^{-/-}$ BMDCs. *Left-hand panel*, control and Raftlin-2 knockdown Raftlin$^{-/-}$ BMDCs were stimulated with 20 μg/ml of polymyxin B-treated poly(I:C). At the indicated time points, IFN-β mRNA expression was analyzed as described above. *Right-hand panel*, mouse Raftlin-2 mRNA expression. Representative data from two independent experiments are shown. *, $p < 0.05$; **, $p < 0.01$. *E*, poly(I:C) cellular uptake by control and Raftlin-2 knockdown Raftlin$^{-/-}$ BMDCs. Representative images from 20 fields in the indicated time points are shown. In Raftlin$^{-/-}$ BMDCs infected with mouse Raftlin-2 shRNA lentiviral particles, 40% of cells fail to internalize poly(I:C) after a 15-min incubation at 37 °C. The number of cells lacking Texas Red/poly(I:C) internalization/total number of cells were for control Raftlin$^{-/-}$ BMDCs, 0/137, and Raftlin-2 knockdown Raftlin$^{-/-}$ BMDCs, 106/260. *Red*, Texas Red/poly(I:C); *blue*, nuclei with DAPI. *Bar*, 5 μm.

localize with CTXB (Fig. 4), whereas in MoDCs it localized to both the plasma membrane and the cytoplasm and membrane-associated Raftlin partially merged with CTXB (Fig. 6*E*). In these cells, poly(I:C) stimulation induced the translocation of Raftlin from the cytoplasm to the plasma membrane where it cooperated with uptake receptor to deliver poly(I:C) to TLR3-positive endosomes (Figs. 4 and 6*F*). Thus, Raftlin is involved in the nucleocapture complex triggering poly(I:C)-mediated TLR3 activation, and appears to act downstream of immune receptors in a cell type-specific manner.

Notably, Raftlin$^{-/-}$ BMDCs that express Raftlin-2 normally took up poly(I:C) (Fig. 7*C*). The expression of Raftlin or Raftlin-2 depends on the cell type. Mouse Raftlin-2 is expressed in B cells but not T cells and is thought to function in a similar way to Raftlin in mouse B cells (33). Because poly(I:C)-induced IFN-β mRNA expression and internalization of poly(I:C) were decreased when mouse Raftlin-2 was knocked down in Raftlin$^{-/-}$ BMDCs (Fig. 7, *D* and *E*), mouse Raftlin-2 participates in poly(I:C) uptake in Raftlin$^{-/-}$ BMDCs. In humans, MoDCs, HEK293 cells, and HeLa cells did not express Raftlin-2 mRNA. Hence, human Raftlin plays a key role in poly(I:C)-induced cellular responses in the absence of Raftlin-2.

The molecular mechanism by which Raftlin cooperates with the uptake receptor to mediate cell entry of poly(I:C) and B- and C-type ODNs is currently unknown. As shown in Fig. 3*A*, clustering of the uptake receptor occurs without internalization in the absence of Raftlin. Because disruption of the lipid raft by treatment with MβCD did not affect internalization of poly(I:C) (supplemental Fig. S4), Raftlin may participate in the assembly of the uptake machinery for poly(I:C) and B- and C-type ODNs independently of lipid raft function. We have previously demonstrated that poly(I:C) is internalized via the clathrin-mediated endocytosis (27). Indeed, Raftlin associated with clathrin after poly(I:C) stimulation (Fig. 5). Thus, Raftlin might be involved in the clathrin and clathrin-associated adapter protein complexes at the plasma membrane and participates in cargo sorting and delivery to the TLR3-positive endosome (34).

Intriguingly, A-type ODN that activates plasmacytoid DCs to induce IFN-α was unable to bind to myeloid DCs (27). A-type ODN binds to high mobility group box 1 and augments the binding of high mobility group box 1 to receptor for advanced glycation end products (35). A-type ODN-high mobility group box 1 complex enhances TLR9-mediated IFN-α production by plasmacytoid DCs in a receptor for advanced glycation end product-dependent manner, although receptor for advanced glycation end products is not essential for internalization of A-type ODN or A-type ODN-high mobility group box 1 complexes. An unidentified uptake receptor for A-type ODN must reside on plasmacytoid DCs. Although whether Raftlin participates in the uptake of A-type ODN in human plasmacytoid DCs remains to be examined, we surmise that exogenous

Downloaded from www.jbc.org at HOKKAIDO DAIGAKU, on May 11, 2011

nucleic acids are recognized by cell surface receptors that form distinct nucleocapture complexes to deliver nucleic acids to intracellular organelles.

The adjuvant activity of poly(I:C) is derived from the activation of two innate immune sensors, TLR3 and MDA5, in myeloid DCs. No RNA molecule has been reported besides poly(I:C) that extracellulary activates either TLR3 or MDA5. Identification of the uptake receptor for poly(I:C) in DCs is important to elucidate the mechanism by which poly(I:C) is localized to TLR3 and MDA5, as well as to develop a poly(I:C)-related adjuvant that is selectively transferred to TLR3 and/or MDA5.

Acknowledgments—We thank Dr. Y. Miyamoto and K. Shida (Osaka Medical Center for Cancer, Osaka, Japan) for technical support and Drs. H. Oshiumi, T. Ebihara, H. Takaki, H. H. Aly, and J. Kasamatsu for invaluable discussions. We also thank Dr. J. P. Atkinson (Washington University) for reviewing this manuscript.

REFERENCES

1. Nagano, Y., and Kojima, Y. (1954) *Compt. Pend. Soc. Biol.* **148,** 1700–1702
2. Lindenmann, J., Burke, D. C., and Isaacs, A. (1957) *Br. J. Exp. Pathol.* **38,** 551–562
3. Field, A. K., Tytell, A. A., Lampson, G. P., and Hilleman, M. R. (1967) *Proc. Natl. Acad. Sci. U.S.A.* **58,** 1004–1010
4. Alexopoulou, L., Holt, A. C., Medzhitov, R., and Flavell, R. A. (2001) *Nature* **413,** 732–738
5. Matsumoto, M., Kikkawa, S., Kohase, M., Miyake, K., and Seya, T. (2002) *Biochem. Biophys. Res. Commun.* **293,** 1364–1369
6. Yoneyama, M., Kikuchi, M., Matsumoto, K., Imaizumi, T., Miyagishi, M., Taira, K., Foy, E., Loo, Y. M., Gale, M., Jr., Akira, S., Yonehara, S., Kato, A., and Fujita, T. (2005) *J. Immunol.* **175,** 2851–2858
7. Kato, H., Takeuchi, O., Sato, S., Yoneyama, M., Yamamoto, M., Matsui, K., Uematsu, S., Jung, A., Kawai, T., Ishii, K. J., Yamaguchi, O., Otsu, K., Tsujimura, T., Koh, C. S., Reis e Sousa, C., Matsuura, Y., Fujita, T., and Akira, S. (2006) *Nature* **441,** 101–105
8. Gitlin, L., Barchet, W., Gilfillan, S., Cella, M., Beutler, B., Flavell, R. A., Diamond, M. S., and Colonna, M. (2006) *Proc. Natl. Acad. Sci. U.S.A.* **103,** 8459–8464
9. Schultz, O., Diebold, S. S., Chen, M., Näslund, T. I., Nolte, M. A., Alexopoulou, L., Azuma, Y. T., Flavell, R. A., Liljeström, P., and Reis e Sousa, C. (2005) *Nature* **433,** 887–892
10. Matsumoto, M., and Seya, T. (2008) *Adv. Drug Deliv. Rev.* **60,** 805–812
11. Kumar, H., Koyama, S., Ishii, K. J., Kawai, T., and Akira, S. (2008) *J. Immunol.* **180,** 683–687
12. McCartney, S., Vermi, W., Gilfillan, S., Cella, M., Murphy, T. L., Schreiber, R. D., Murphy, K. M., and Colonna, M. (2009) *J. Exp. Med.* **206,** 2967–2976
13. Miyake, T., Kumagai, Y., Kato, H., Guo, Z., Matsushita, K., Satoh, T., Kawagoe, T., Kumar, H., Jang, M. H., Kawai, T., Tani, T., Takeuchi, O., and Akira, S. (2009) *J. Immunol.* **183,** 2522–2528
14. Longhi, M. P., Trumpfheller, C., Idoyaga, J., Caskey, M., Matos, I., Kluger, C., Salazar, A. M., Colonna, M., and Steinman, R. M. (2009) *J. Exp. Med.* **206,** 1589–1602
15. Ebihara, T., Azuma, M., Oshiumi, H., Kasamatsu, J., Iwabuchi, K., Matsumoto, K., Saito, H., Taniguchi, T., Matsumoto, M., and Seya, T. (2010) *J. Exp. Med.* **207,** 2675–2687
16. Matsumoto, M., Funami, K., Tanabe, M., Oshiumi, H., Shingai, M., Seto, Y., Yamamoto, A., and Seya, T. (2003) *J. Immunol.* **171,** 3154–3162
17. Funami, K., Sasai, M., Ohba, Y., Oshiumi, H., Seya, T., and Matsumoto, M. (2007) *J. Immunol.* **179,** 6867–6872
18. Oshiumi, H., Matsumoto, M., Funami, K., Akazawa, T., and Seya, T. (2003) *Nat. Immunol.* **4,** 161–167
19. Yamamoto, M., Sato, S., Hemmi, H., Hoshino, K., Kaisho, T., Sanjo, H., Takeuchi, O., Sugiyama, M., Okabe, M., Takeda, K., and Akira, S. (2003) *Science* **301,** 640–643
20. Kawai, T., Takahashi, K., Sato, S., Coban, C., Kumar, H., Kato, H., Ishii, K. J., Takeuchi, O., and Akira, S. (2005) *Nat. Immunol.* **6,** 981–988
21. Seth, R. B., Sun, L., Ea, C. K., and Chen, Z. J. (2005) *Cell* **122,** 669–682
22. Meylan, E., Curran, J., Hofmann, K., Moradpour, D., Binder, M., Bartenschlager, R., and Tschopp, J. (2005) *Nature* **437,** 1167–1172
23. Xu, L. G., Wang, Y. Y., Han, K. J., Li, L. Y., Zhai, Z., and Shu, H. B. (2005) *Mol. Cell* **19,** 727–740
24. Lee, H. K., Dunzendorfer, S., Soldau, K., and Tobias, P. S. (2006) *Immunity* **24,** 153–163
25. Limmon, G. V., Arredouani, M., McCann, K. L., Corn Minor, R. A., Kobzik, L., and Imani, F. (2008) *FASEB J.* **22,** 159–167
26. Krieg, A. M. (2002) *Annu. Rev. Immunol.* **20,** 709–760
27. Itoh, K., Watanabe, A., Funami, K., Seya, T., and Matsumoto, M. (2008) *J. Immunol.* **181,** 5522–5529
28. Ranjith-Kumar, C. T., Duffy, K. E., Jordan, J. L., Eaton-Bassiri, A., Vaughan, R., Hoose, S. A., Lamb, R. J., Sarisky, R. T., and Kao, C. C. (2008) *Mol. Cell. Biol.* **28,** 4507–4519
29. Saeki, K., Miura, Y., Aki, D., Kurosaki, T., and Yoshimura, A. (2003) *EMBO J.* **22,** 3015–3026
30. Obuse, C., Iwasaki, O., Kiyomitsu, T., Goshima, G., Toyoda, Y., and Yanagida, M. (2004) *Nat. Cell Biol.* **6,** 1135–1141
31. Ebihara, T., Shingai, M., Matsumoto, M., Wakita, T., and Seya, T. (2008) *Hepatology* **48,** 48–58
32. Ding, C., Wang, L., Al-Ghawi, H., Marroquin, J., Mamula, M., and Yan, J. (2006) *Eur. J. Immunol.* **36,** 2013–2024
33. Saeki, K., Fukuyama, S., Ayada, T., Nakaya, M., Aki, D., Takaesu, G., Hanada, T., Matsumura, Y., Kobayashi, T., Nakagawa, R., and Yoshimura, A. (2009) *J. Immunol.* **182,** 5929–5937
34. Ohno H. (2006) *J. Cell Sci.* **119,** 3719–3721
35. Tian, J., Avalos, A. M., Mao, S. Y., Chen, B., Senthil, K., Wu, H., Parroche, P., Drabic, S., Golenbock, D., Sirois, C., Hua, J., An, L. L., Audoly, L., La Rosa, G., Bierhaus, A., Naworth, P., Marshak-Rothstein, A., Crow, M. K., Fitzgerald, K. A., Latz, E., Kiener, P. A., and Coyle, A. J. (2007) *Nat. Immunol.* **8,** 487–496

Downloaded from www.jbc.org at HOKKAIDO DAIGAKU, on May 11, 2011

Molecular Immunology 48 (2011) 497–504

Contents lists available at ScienceDirect

Molecular Immunology

journal homepage: www.elsevier.com/locate/molimm

Strain-to-strain difference of V protein of measles virus affects MDA5-mediated IFN-β-inducing potential

Hiromi Takaki[1], Yumi Watanabe[1], Masashi Shingai[2], Hiroyuki Oshiumi, Misako Matsumoto, Tsukasa Seya*

Department of Microbiology and Immunology, Graduate School of Medicine, Hokkaido University, Kita-ku, Sapporo 060-8638, Japan

ARTICLE INFO

Article history:
Received 22 June 2010
Received in revised form 7 October 2010
Accepted 12 October 2010
Available online 10 November 2010

Keywords:
Measles virus
V protein
MDA5
IRF-3
Interferon-beta

ABSTRACT

Laboratory-adapted and vaccine strains of measles virus (MV) induce type I interferon (IFN) in infected cells to a far greater extent than wild-type strains. We investigated the mechanisms for this differential type I IFN production in cells infected with representative MV strains. The overexpression of the wild-type V protein suppressed melanoma differentiation-associated gene 5 (MDA5)-induced IFN-β promoter activity, while this was not seen in A549 cells expressing CD150 transfected with the V protein of the vaccine strain. The V proteins of the wild-type also suppressed poly I:C-induced IFN regulatory factor 3 (IRF-3) dimerization. The V proteins of the wild-type and vaccine strain did not affect retinoic acid-inducible gene 1 (RIG-I)- or toll-IL-1R homology domain-containing adaptor molecule 1 (TICAM-1)-induced IFN-β promoter activation. We identified an amino acid substitution of the cysteine residue at position 272 (which is conserved among paramyxoviruses) to an arginine residue in the V protein of the vaccine strain. Only the V protein possessing the 272C residue binds to MDA5. The mutation introduced into the wild-type V protein (C272R) was unable to suppress MDA5-induced IRF-3 nuclear translocation and IFN-β promoter activation as seen in the V proteins of the vaccine strain, whereas the mutation introduced in the vaccine strain V protein (R272C) was able to inhibit MDA5-induced IRF-3 and IFN-β promoter activation. The other 6 residues of the vaccine strain V sequence inconsistent with the authentic sequence of the wild-type V protein barely affected the IRF-3 nuclear translocation. These data suggested that the structural difference of vaccine MV V protein hampers MDA5 blockade and acts as a nidus for the spread/amplification of type I IFN induction. Ultimately, measles vaccine strains have two modes of IFN-β-induction for their attenuation: V protein mutation and production of defective interference (DI) RNA.

© 2010 Elsevier Ltd. All rights reserved.

1. Introduction

Innate immunity is the first line of defense against virus infection, and the most powerful antiviral agent possessed by the host immune system is interferon (IFN). Expression of type I IFN in host cells induces a set of IFN-inducible genes which efficiently suppress viral replication and spread (Pichlmair and Reis, 2007). Host cells usually terminate virus replication in response to IFN induction. Recent studies elucidated the mechanism by which type I IFN is induced and found that it senses virus patterns such as 5′-triphosphate (5′-3P) and stem-loops or double-stranded RNA (dsRNA) (Takeuchi and Akira, 2008). dsRNA specifically is present in several forms: viral genomes, single-stranded RNA virus replication intermediates, DNA virus symmetrical transcription products, defective viral particles and debris from lysed cells (Bowie and Fitzgerald, 2007). These viral products all present patterns that activate the IFN system. In fact, extracellular dsRNA is sensed by endosomal Toll-like receptor 3 (TLR3), and intracellular dsRNA is detected by cytoplasmic RNA helicase retinoic acid-inducible gene 1 (RIG-I) and melanoma differentiation-associated gene 5 (MDA5) (Takeuchi and Akira, 2008). TLR3 recruits the adaptor, toll-IL-1R homology domain-containing adaptor molecule 1 (TICAM-1, also named TRIF) (Oshiumi et al., 2003). RIG-I and MDA5 signal through IFN-β promoter stimulator 1 (IPS-1). These adaptor molecules activate kinase TANK-binding kinase I (TBK1), inhibitor of κB kinase ε (IKKε) and NAK-associated protein 1 (NAP-1) (Sasai et al., 2006a). These complexes then phosphorylate IFN regulatory factor 3 (IRF-

* Corresponding author at: Department of Microbiology and Immunology, Graduate School of Medicine, Hokkaido University, Kita 15, Nishi 7, Kita-ku, Sapporo 060-8638, Japan. Tel.: +81 11 706 7866; fax: +81 11 706 7866.
E-mail address: seya-tu@pop.med.hokudai.ac.jp (T. Seya).
[1] First two authors equally contributed to this work.
[2] Present address: Laboratory of Molecular Microbiology, National Institute of Allergy and Infectious Diseases, National Institutes of Health, Bethesda, MD 20892.

0161-5890/$ – see front matter © 2010 Elsevier Ltd. All rights reserved.
doi:10.1016/j.molimm.2010.10.006

3) and IRF-7, promoting their dimerization, nuclear translocation and transcription of IFN-stimulated genes (ISGs), such as ISG56, as well as IFN and other cytokines (Medzhitov, 2007; Platanias, 2005). On the other hand, secreted IFNs bind to the IFN-α/β receptor on the surface of adjacent cells and activate the Janus kinase–signal transducer and activator of transcription (JAK/STAT) signaling pathway, which amplifies IFN induction and stimulates transcription of a variety of antiviral genes (Samuel, 2001). Many viruses encode specific proteins to inhibit IFN induction or the JAK/STAT pathway (Katze et al., 2002; Sen, 2001). The V protein of measles virus (MV) blocks the IFN-inducing pathway mediated by MDA5 and the JAK/STAT pathway (Ohno et al., 2004; Nakatsu et al., 2008). The C protein of MV acts as a regulator of viral RNA synthesis, thereby acting indirectly to suppress IFN induction (Nakatsu et al., 2008).

It has been reported that wild-type measles strains barely induce type I IFN (Naniche et al., 2000; Shingai et al., 2007). The levels of IFN protein or mRNA are lower than the detection limit in cells infected with wild-type MV, while higher levels of IFN are detectable in cells infected with vaccine strains. Although the mechanism behind the strain-to-strain differences in IFN-inducing potential remain unclear, an early report suggested that a laboratory strain, strain Edmonston (ED), possesses a unique V protein with low suppression of IFN-α/β receptor (IFNAR)-amplifiable IFN induction (Ohno et al., 2004). We previously reported that vaccine/laboratory strains harbor defective interference (DI) RNA which activates RIG-I and/or MDA5. Type I IFN is efficiently yielded by DI RNA during viral RNA replication (Shingai et al., 2007). We found that the majority of measles vaccine and laboratory-adapted strains possess DI RNA. However, the IFN-inducibility of attenuated MV strains does not always correlate with the presence of DI RNA. Therefore, the mechanisms by which the primary IFN-inducing activity by RIG-I/MDA5 is impaired during wild-type measles infection still remain unexplained.

In this study, using wild-type and DI-negative attenuated measles strains, we investigated the predominate mechanisms that act on the host IFN system to modulate IFN production. We identified amino acid differences between the V proteins of the attenuated ED strain and wild-type MV, and found that the cysteine residue at position 272 (272C) was required for suppression of MDA5-induced type I IFN production.

2. Materials and methods

2.1. Cell culture and reagents

The human lung epithelial cell line (A549), A549/CD150, African green monkey kidney cell line (Vero), Vero/CD150 and HEK293FT cells were maintained in DMEM supplemented with 10% heat-inactivated FCS and antibiotics (Tanabe et al., 2003). HeLa cells were cultured in Eagle's MEM with 10% heat-inactivated FCS and L-glutamine. For establishing CD150-expressing A549 and Vero cell lines, pCNX2-huCD150 was introduced into cell lines using FugeneHD (Roche) according to the manufacturer's protocol. Twenty-four hours after transfection, the neomycin analog G418 (Sigma–Aldrich) was added to the medium at the final concentration of 1.4 mg/ml or 0.6 mg/ml for Vero or A549 cells. During selection, G418-containing medium was changed once every 4 days. G418-resistant, stably transfected clones were propagated for the study of surface expression of CD150 by flow cytometer. The following antibodies were obtained commercially: anti-FLAG (Sigma–Aldrich); anti-Myc (Santa Cruz); anti-IRF-3 (IBL). Alexa Fluor 488- and Alexa Fluor 568-conjugtaed secondary antibodies were from Invitrogen Life Technologies. Polyriboinosinic/polyribocytidylic acid (polyI:C) was from Amersham Biosciences.

2.2. Plasmids

Complementary DNAs of human TICAM-1, MDA5, RIG-I, V and C were cloned in our laboratory by RT-PCR and ligated into the cloning site of the expression vector, pEF-BOS, pcDNA4 Myc-HisA and pCMV10-FLAG (Funami et al., 2008). Mutations were introduced by site-directed mutagenesis using PCR. All constructs were confirmed by sequencing.

2.3. Virus preparation and titration

Nagataha (NV) and Edmonston (ED) strains were obtained from Dr. S. Ueda (the Research Institute for Microbial Diseases, Osaka University, Osaka, Japan) and University of Washington (Seattle, WA), respectively. Ichinose (IC)-B was provided from Dr. F. Kobune (National Institutes of Health, Tokyo, Japan) (Kubune et al., 1990). Masusako (MS) was propagated in our laboratory (Kurita-Taniguchi et al., 2000; Murabayashi et al., 2002). NV, ED and MS strains were maintained in Vero/CD150 cells in our laboratory (Shingai et al., 2007). IC-B strain was maintained in B95a cells. Virus titer was determined as PFUs on Vero/CD150 and the multiplicity of the infection (MOI) of each experiment was calculated based on this titer (Kubune et al., 1990).

2.4. RT-PCR and real-time PCR

Total RNA was prepared using TRIzol Reagent (Invitrogen) following the manufacturer's instructions. RT-PCR was carried out using the High Capacity cDNA Reverse Transcription kit (Applied Biosystems) according to the manufacturer's instructions. The following oligonucleotides were used for human GAPDH: 5′-TCCACCACCCTGTTGCTGTA-3′ and 5′-ACCACAGTCCATGCCATCAC-3′; and for MV-H: 5′-CCCTTATCAACGGATGATCC-3′ and 5′-GTGATCAATGGCCCCAATCC-3′; and for q-PCR human β-actin: 5′-CCTGGCACCCAGCACAAT-3′ and 5′-GCCGATCCACACGGAGTACT-3′; and for *q*-PCR human IFN-β: 5′-CAATTGCTTGGATTCCTACAAAG-3′ and 5′-TATTCAAGCCTCCCATTCAATTG-3′. IFN-β mRNA were normalized to β-actin and fold inductions of transcripts were calculated using the ddCT method relative to unstimulated HeLa cells.

2.5. RT-PCR amplification of cDNA from 5′ copy-back DI RNAs

We modified the RT-PCR amplification protocol of Calain et al. (1992), where the copy-back DI RNAs were amplified using two set of MV primers (for 5′ copy-back DIs, JM396; 5′-TATAAGCTTACCAGACAAAGCTGGGAATAGAAACTTCG-3′/JM403; 5′-CGAAGATATTCTGGTGTAAGTCTAGTA-3′, and for standard genome, JM396/JM402; 5′-TTTATCCAGAATCTCAARTCCGG-3′) (Sidhu et al., 1994; Whistler et al., 1996). Viral RNA from the culture supernatant was extracted with QIAamp Viral RNA Mini kit (Qiagen). Total RNA from viral-infected cells was extracted with TRIzol Reagent following the manufacturer's instructions. RT-PCR was carried out using the High Capacity cDNA Reverse Transcription kit (Applied Biosystems) according to the manufacturer's instructions. The PCR-amplified products were confirmed by sequencing.

2.6. Reporter gene assay

Cells were seeded onto 24-well plates and transfected with various amounts of expression vectors, the reporter gene, and the phRL-TK control plasmid using FuGene HD (Roche) according to the manufacturer's instructions. After 24 h, the cells were harvested in 100 μl lysis buffer. The luciferase activity was measured using Dual-